University of Twente

EEMCS / Electrical Engineering
Robotics and *Mechatronics*

Control Strategy for Variable Gait using Variable Knee Stiffness in a Bipedal Robot Model

W. (Wesley) Roozing

MSc Report

Committee:
Prof.dr.ir. S. Stramigioli
Dr. R. Carloni
E. Barrett, MSc
Prof.dr.ir. H. van der Kooij

January 2014

Report nr. 002RAM2014
Robotics and Mechatronics
EE-Math-CS
University of Twente
P.O. Box 217
7500 AE Enschede
The Netherlands

John Cleese, The Ministry of Silly Walks

Contents

1 Introduction

The work described in this master thesis investigates the control of bipedal walking robots based on the principle of passive dynamic walking. Inspired by the high performance of human walking, which combines high robustness with high energy efficiency, the goal has been to use variable leg stiffness to obtain variable walking gait while combining these two aspects. In contrast, most existing systems are either energy efficient or robust.

The thesis consists mainly of two papers; the first investigates the use of variable leg stiffness to obtain variable gait on the Spring-Loaded Inverted Pendulum (SLIP) model. The parameter space in which gaits of a desired velocity exist is first explored and a normalised unique description of a SLIP gait is developed. Based on the control of variable leg stiffness, a gait switching strategy is proposed that controls the system from one limit cycle walking gait to another in order to change the walking speed. The strategy is shown to be able to control the system to another gait within a limited number of steps, after which control action converges to zero.

The second paper investigates the Segmented Spring-Loaded Inverted Pendulum (S-SLIP) model, which is different from the SLIP model in that it has legs with torsional stiffness knees, which is more realistic as compared to existing robot designs, which use knees and leg retraction to avoid food scuffing. It is shown that the S-SLIP model exhibits walking gait, and a control strategy is developed that is able to stabilise the system after a disturbance. The gait switching strategy is applied to this model and it is shown that the system can be controlled from one limit cycle walking gait to another.

Furthermore, a realistic bipedal robot model is designed that uses Variable Stiffness Actuators (VSAs) to control the knee stiffness. The control is based on the strategy developed for the S-SLIP model, and is extended with additional components to facilitate hip swing and leg retraction, which arise due to the additional dynamics of this model. A reference gait is obtained by using this model with constant leg stiffness. The variable knee stiffness is then used to stabilise the system into this gait and to inject energy losses generated by foot impacts. It is shown that this results in a stable limit cycle walking gait. The thesis concludes with a discussion of results obtained and recommendations for future work.

2 Paper 1: Variable Bipedal Walking Gait with Variable Leg Stiffness

Submitted to ICRA 2014.

Abstract – The Spring-Loaded Inverted Pendulum (SLIP) model has been shown to exhibit many properties of human walking, and therefore has been the starting point for studies on robust, energy-efficient walking for robots. We address the problem of online gait variation on the SLIP model by control of the leg stiffness and adjustment of the angle-of-attack in order to switch between gaits and thus regulate walking speeds. We show that it is possible to uniquely describe SLIP limit cycle gaits in fully normalised form. Using that description, we propose both an instantaneous switching method and an interpolation method with an optimisation step to switch between limit cycle SLIP gaits. Using simulations, we show that it is then possible to transition between them online, after which the system converges back to zero-input limit cycle walking.

Variable Bipedal Walking Gait with Variable Leg Stiffness

W. Roozing, L.C. Visser, and R. Carloni

***Abstract*— The Spring-Loaded Inverted Pendulum (SLIP) model has been shown to exhibit many properties of human walking, and therefore has been the starting point for studies on robust, energy-efficient walking for robots. We address the problem of online gait variation on the SLIP model by control of the leg stiffness and adjustment of the angle-of-attack in order to switch between gaits and thus regulate walking speeds. We show that it is possible to uniquely describe SLIP limit cycle gaits in fully normalised form. Using that description, we propose both an instantaneous switching method and an interpolation method with an optimisation step to switch between limit cycle SLIP gaits. Using simulations, we show that it is then possible to transition between them online, after which the system converges back to zero-input limit cycle walking.**

I. INTRODUCTION

This work is inspired by the high performance of human walking, which combines high robustness with high energy efficiency. In contrast, most existing legged robotic systems show either high robustness or energy efficiency.

Passive dynamic walking can be realised by designing mechanics such that it has a walking gait as dynamic mode [1]. However, while designs based on the principle of passive dynamic walking show high energy efficiency, they are not very robust against external disturbances. Other, highly controlled systems show high robustness at the exchange of energy efficiency [2]. Combining these two aspects has proven difficult. Furthermore, these robots rely on compass gaits, using either stiff legs or locking the knee during walking, which does not resemble human legs.

It has been shown that human walking on flat terrain can be accurately modeled by an inverted passive mass-spring system. The Spring-Loaded Inverted Pendulum (SLIP) model shows walking dynamics strongly comparable to human walking in terms of hip trajectory, single- and double-support phases and ground contact forces [3]. It exhibits self-stable walking and running gait for a relatively large range of system parameters. It can demonstrate walking with different forward velocities as well as running [3], [4]. Although the SLIP model exhibits self-stable walking gait for large ranges of parameters on its own, it has been shown that the basin of attraction can be enlarged by control of a variable leg stiffness [5]. The Variable SLIP (V-SLIP) model significantly increases robustness against external disturbances and, after a disturbance, is able to restabilise the system into its original gait by injecting or removing energy appropriately.

It is very desirable to be able to change the forward velocity of legged robots, for example slowing down to save energy, or speeding up to travel large distances quickly. In [6], it was shown that it is possible to change gait on the SLIP model by controlling the angle-of-attack. However, the method relies on imposing constant system energy, thus significantly reducing achievable velocities by injecting or removing energy in the system. In [7], the authors propose velocity control of a four-link walking model with stiff legs by changing step length and the frequency of the hip actuation. By placing their robot on a slope, they negate the loss of energy due to foot impacts and propose a velocity control strategy by controlling the slope. The work done in [8] shows in simulation and experiment that it is possible to change velocity by changing step length and joint stiffnesses. They use variable stiffness actuators in each joint, but lock the stance leg knee to support the robot. A stiff-legged walker is also used in [9], but the authors vary the pitch of a torso to induce different walking speeds. These works rely on compass gaits, using either stiff legs or locked knees during stance.

The problem of online gait variation is addressed in this work by the design of a control strategy for the V-SLIP model that allows to switch between limit cycle gaits during walking by actively controlling the leg stiffness and angle-of-attack. We propose an optimisation criterion that aligns the two gaits and then switches between them by changing control references and system parameters appropriately, after which the system converges back to zero-input limit cycle walking. Energy is injected or removed from the system appropriately to accommodate the new gait.

The remainder of this paper is outlined as follows. Section II describes the SLIP model. Also, a normalised notation of SLIP limit cycle gaits is introduced. Section III outlines the control strategy to control the V-SLIP system and switch between limit cycle gaits. Section V contains simulation results of the proposed method. Lastly, Section VI concludes on the work and proposes directions for future efforts.

II. THE SPRING-LOADED INVERTED PENDULUM (SLIP) MODEL

A. SLIP Dynamics

The bipedal Spring-Loaded Inverted Pendulum (SLIP) model is shown in Fig. 1. It consists of a hip point mass m, which connects two massless telescopic legs. The legs consist of springs with rest length L_0 and stiffnesses $k_1 = k_2 = k_0$. Given properly chosen initial conditions, the SLIP model shows stable passive walking gaits [3], [4].

1) Configuration Manifold & State Transitions: The configuration of the system is given by the position of the hip mass as $(x, y) =: \mathbf{q} \in \mathcal{Q}$, and its velocity by $\dot{\mathbf{q}} \in T_{\mathbf{q}}\mathcal{Q}$,

W. Roozing and R. Carloni are with the Robotics And Mechatronics group, MIRA Institute, University of Twente, The Netherlands. E-mail: w.roozing@student.utwente.nl, r.carloni@utwente.nl

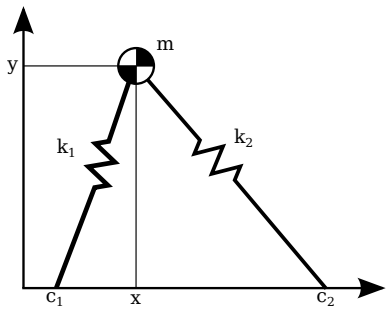

Fig. 1. The SLIP model consists of a hip point mass m, with two massless telescopic springs with stiffnesses $k_1 = k_2 = k_0$ as legs. The model is shown during double-support phase, with both legs touching the ground at contact points c_1 and c_2.

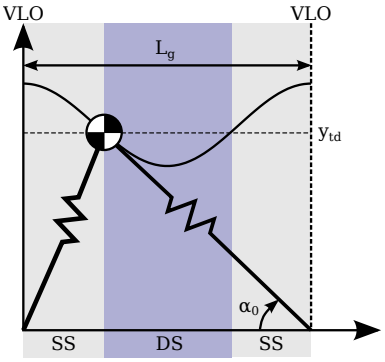

Fig. 2. A single step of the SLIP model, shown at the moment of touchdown. The step starts and ends at VLO and has length L_g. Note that at touchdown, the swing leg is at exactly α_0 with the ground and has length L_0. At touchdown, the SLIP model goes into double-support (DS) phase, shown by the touch-down height y_{td}, and returns into single-support (SS) phase when the hip again crosses y_{td} and the trailing leg reaches length L_0.

the tangent space to $\mathcal{Q}$ at $\mathbf{q}$. The system state is then given as $\mathbf{x} := (\mathbf{q}, \mathbf{p})$, with the momentum $\mathbf{p} := (p_x, p_y) = M\dot{\mathbf{q}}$ and the mass matrix $M = \mathrm{diag}(m, m)$. A single step is defined as a trajectory $\mathbf{q}(t) \in \mathcal{Q}$ that starts with the system in Vertical Leg Orientation (VLO), where the hip mass is exactly above the supporting leg. The step ends when the system again reaches VLO (Fig. 2), and the role of the legs is then exchanged. We define the gait length $L_g := x(T)$, i.e. the distance travelled after one step, where T is the gait time period.

During a single step, two phases must be distinguished – single-support (SS) and double-support (DS), during which one and two legs are in touch with the ground respectively. The transition from single- to double-support occurs when the mass reaches the touch-down height y_{td} associated with the angle-of-attack α_0 and the swing leg touches the ground (Fig. 2):

$$y = y_{td} := L_0 \sin(\alpha_0) \tag{1}$$

The location of the leading contact point c_2 is then calculated as (Fig. 1):

$$c_2 = x + L_0 \cos(\alpha_0) \tag{2}$$

Similarly, the transition from double- to single-support occurs when either leg reaches its rest length:

$$\sqrt{(x - c_i)^2 + y^2} = L_0\,, \quad i \in \{1, 2\} \tag{3}$$

At transition to single-support, the swing leg disappears and reappears at the subsequent instance of touch-down, which is possible because the leg is massless. In the nominal case, only the trailing leg reaches its rest length and contact c_2 is relabeled as c_1 to correspond to the notation used during single-support phase. We can now define two subsets of $\mathcal{Q}$ which correspond to the single- and double-support phases respectively:

$$\begin{aligned} \mathcal{Q}_{SS} &= \{\mathbf{q} \in \mathcal{Q} \,|\, y > y_{td}\,,\; y < L_0\} \\ \mathcal{Q}_{DS} &= \{\mathbf{q} \in \mathcal{Q} \,|\, y < y_{td}\,,\; y > 0\} \end{aligned} \tag{4}$$

where $y < L_0$ and $y > 0$ are included to avoid the remaining cases, i.e. lift-off and fall respectively. Note that for a walking gait $\mathbf{q} \in \mathcal{Q}_{SS} \cup \mathcal{Q}_{DS}$. [1]

2) System Dynamics: To derive the dynamic equations for the system, we use the Hamiltonian approach. The kinetic energy function is defined as $K = \frac{1}{2}\mathbf{p}^T M^{-1}\mathbf{p}$ and the potential energy function as

$$V = mgy + \frac{1}{2}k_0\left(L_0 - L_1\right)^2 + \frac{1}{2}k_0\left(L_0 - L_2\right)^2$$

where $L_i = \sqrt{(x - c_i)^2 + y^2}$ and g is the gravitational acceleration. During single-support phase, we set $L_2 \equiv L_0$, i.e. the swing leg is uncompressed and it exerts no force. The dynamic equations are then defined by the Hamiltonian energy function $H = K + V$ as

$$\frac{\mathrm{d}}{\mathrm{d}t}\begin{bmatrix}\mathbf{q}\\ \mathbf{p}\end{bmatrix} = \begin{bmatrix}0 & I\\ -I & 0\end{bmatrix}\begin{bmatrix}\frac{\delta H}{\delta \mathbf{q}}\\ \frac{\delta H}{\delta \mathbf{p}}\end{bmatrix} \tag{5}$$

Note that a solution $\mathbf{q}(t)$ of (5) is of class C^2, due to the non-differentiability of the leg forces at the moment of transition between the single- and double-support phases.

B. Limit Cycle Gaits for the SLIP Model

It was shown [4] that, given the proper system parameters and initial conditions, the dynamics described by (5) exhibit autonomous stable walking gait. A limit cycle gait is a periodic walking gait which returns to the same state periodically. From this point on, we refer to limit cycle gaits of the SLIP model as *natural gaits*.

In our description of natural gaits we use the state at VLO as initial conditions, i.e. $\mathbf{x}_0 = (\mathbf{q}, \mathbf{p})_0 = (x, y, p_x, p_y)_0$, and, during walking in natural gait, the system returns to this state at every VLO. Since we can take at VLO $x \equiv 0$, a natural gait can then be fully described as

$$\Sigma = (\alpha_0, k_0, L_0, m, y_0, p_{x,0}, p_{y,0}) \tag{6}$$

[1] Lift-off is also possible while $\mathbf{q} \in \mathcal{Q}_{SS} \cup \mathcal{Q}_{DS}$. We take care of this in simulation by checking $L_1 \leq L_0 \vee L_2 \leq L_0$, i.e. there is always at least one leg in contact with the ground.

Note that it is not possible to use the total system energy H to uniquely describe a natural gait, because energy can be stored in either potential or kinetic energy.

C. A Normalised Notation of SLIP Limit Cycle Gaits

k_0 and H can be normalised, such that SLIP models with different parameters can be compared easily:

$$\tilde{k} = k_0 \frac{L_0}{mg} \qquad \tilde{H} = \frac{H}{L_0 mg} \tag{7}$$

If we normalise $\mathbf{x}$ as $\tilde{\mathbf{x}} := (\tilde{\mathbf{q}}, \tilde{\mathbf{p}}) = (\tilde{x}, \tilde{y}, \tilde{p}_x, \tilde{p}_y)$ with

$$\tilde{x} = \frac{x}{L_0} \quad \tilde{y} = \frac{y}{L_0} \quad \tilde{p}_x = \frac{p_x}{m\sqrt{L_0 g}} \quad \tilde{p}_y = \frac{p_y}{m\sqrt{L_0 g}} \tag{8}$$

and use (7), we obtain a fully normalised unique description $\tilde{\Sigma}$ of a natural gait:

$$\tilde{\Sigma} = \left(\alpha_0, \tilde{k}, \tilde{y}_0, \tilde{p}_{x,0}, \tilde{p}_{y,0}\right) \tag{9}$$

The gait trajectory can then be found by solving (5) for $\tilde{\Sigma}$. Using this description, equal gaits on different SLIP systems now result in the same normalised state trajectory $\tilde{\mathbf{x}}(t) = (\tilde{\mathbf{q}}(t), \tilde{\mathbf{p}}(t))$. Similarly to $\tilde{p}_x, \tilde{p}_y$, the velocities are normalised as

$$\dot{\tilde{x}} = \frac{\dot{x}}{\sqrt{L_0 g}} \qquad \dot{\tilde{y}} = \frac{\dot{y}}{\sqrt{L_0 g}} \tag{10}$$

Note that the normalisation $\dot{\tilde{x}}$ is the Froude number Fr [8], [9], used to compare the relative walking speeds of systems with different leg lengths.

III. CONTROL DESIGN

By actively controlling the leg stiffness of the SLIP model, the robustness of the system to external disturbances can be significantly increased and, after a disturbance, the system can be stabilised into its original gait by injecting or removing energy appropriately [5]. The extended model, called Variable-SLIP (V-SLIP), replaces the constant stiffness legs by variable stiffness legs.

We use the ability to change the leg stiffness to transition between gaits. The rationale is as follows. By considering a gait switch as a disturbance to the system which has to be rejected, the system can be controlled into any gait which is within the basin of attraction of the closed loop system. Furthermore, because there are large continuous regions of self-stable natural gaits with different forward velocities [4], the system can change into nearly any gait by using an appropriate transition strategy. In this section, we discuss the leg stiffness control that stabilises the system into a natural gait. The next section will discuss the gait transition strategy.

The variable stiffness legs of the V-SLIP model have stiffness $k_i = k_0 + u_i$, with control inputs u_i restricted to subsets $U_i = \{u_i \in \mathbb{R} \mid 0 < k_0 + u_i < \infty\}$, such that the result is physically meaningful. Given a natural SLIP gait $\tilde{\Sigma}$ and corresponding state trajectory $\tilde{\mathbf{x}}(t)$, which is a solution of (5), we intend to control the system such that it converges to its natural gait, i.e. a reference $\tilde{\mathbf{x}}^\circ(t)$ such that $u_i \to 0$ and $k_i \to k_0$, $i \in \{1, 2\}$. However, as the system is underactuated during the single-support phase, these references cannot be tracked exactly, and as the system lags behind the reference this may lead to instability. Because $\tilde{x}$ was identified as a periodic variable, and required to be monotonically increasing in time, the references may be reparametrised in $\tilde{x}$. Due to the parametrisation in $\tilde{x}$, the gait references are sufficiently described as

$$\tilde{y}^*(\tilde{x}) = \tilde{y}^o(\tilde{x}) \qquad \dot{\tilde{x}}^*(\tilde{x}) = \dot{\tilde{x}}^o(\tilde{x}) \tag{11}$$

However, as a general analytic expression for the spring-loaded pendulum does not exist [10], a Fourier series expansion approximation of the numerical solution is used.

To formulate the control strategy, we rewrite Eq. (5) in standard form as

$$\dot{\mathbf{x}} = f(\mathbf{x}) + \sum_i g_i(\mathbf{x}) u_i \tag{12}$$

and then define error functions h_1 and h_2 as

$$\begin{aligned} h_1 &= y - y^* \\ h_2 &= \dot{x} - \dot{x}^* \end{aligned} \tag{13}$$

The control solution is then given as follows.

- For $\mathbf{q} \in \mathcal{Q}_{SS}$:

$$\begin{aligned} u_1 &= \frac{1}{L_{g_1} L_f h_1} \left(-L_f^2 h_1 - \kappa_d L_f h_1 - \kappa_p h_1\right) \\ u_2 &\equiv 0 \end{aligned} \tag{14}$$

- For $\mathbf{q} \in \mathcal{Q}_{DS}$:

$$\begin{bmatrix} u_1 \\ u_2 \end{bmatrix} = A^{-1} \begin{bmatrix} -L_f^2 h_1 - \kappa_d L_f h_1 - \kappa_p h_1 \\ -L_f h_2 - \kappa_v h_2 \end{bmatrix} \tag{15}$$

with

$$A = \begin{bmatrix} L_{g_1} L_f h_1 & L_{g_2} L_f h_1 \\ L_{g_1} L_f h_2 & L_{g_2} L_f h_2 \end{bmatrix} \tag{16}$$

where $L_f^2 h_i$, $L_f h_i$ and $L_{g_i} L_f h_i$ denote the (repeated) Lie-derivatives of h_i along the vector fields defined in (12) and $\kappa_d, \kappa_p, \kappa_v$ are tunable control parameters. The control inputs (14), (15) ensure that the error h_1 converges asymptotically to zero and that the error h_2 is at least bounded [5].

Remark: Due to the structure of the problem, the system is not fully controllable during the single-support phase. Because the error in y influences touch-down and lift-off events, it is deemed more important. Thus, by design, only h_1 is controlled during the single-support phase (Eq. (14)).

Remark: During either single- or double-support, the control inputs u_1 and u_2 are continuous. However, their continuity is not guaranteed at the moment of phase transition.

IV. GAIT TRANSITION

A. Search of Stable Gaits

Suppose the system described by the SLIP model is in some natural gait and it is commanded to change the velocity. As natural gaits exist for large ranges of parameters, there often exists a range of natural gaits that achieve that velocity. This is shown in Fig. 3. Natural gaits exist for many values of $(\alpha_0, \tilde{k})$, and a single set $(\alpha_0, \tilde{k})$ can in general achieve a range of average forward velocities (vertical bar in Fig. 3).

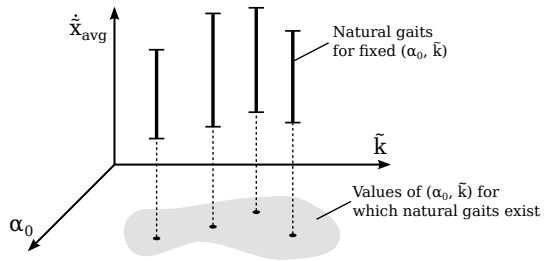

Fig. 3. Average forward velocities $\dot{\tilde{x}}_{avg}$ of natural gaits for different values of $(\alpha_0, \tilde{k})$. Note that for given $(\alpha_0, \tilde{k})$, the average forward velocity is proportional to the system energy $\tilde{H}$.

In choosing $(\alpha_0, \tilde{k})$, there may be practical design considerations. The range of stiffnesses obtainable in practice is limited, and the range of acceptable angles of attack is limited due to foot slip and energy loss due to high ground impact forces and so forth. Exactly which values of $(\alpha_0, \tilde{k})$ are chosen is arbitrary within the ranges of natural gaits. The next sections describe a general method for switching from some given gait $\tilde{\Sigma}_i$ to some other given gait $\tilde{\Sigma}_j$, independently of $\tilde{\Sigma}_i$ and $\tilde{\Sigma}_j$. We do, however, make a distinction between switching between gaits with equal values of $(\alpha_0, \tilde{k})$ (Section IV-C.1) and gaits with different $(\alpha_0, \tilde{k})$ (Section IV-C.2).

B. Optimisation Criterion for Gait Switching

1) Finding Optimal Points: Suppose that two natural gaits $\tilde{\Sigma}_i$ and $\tilde{\Sigma}_j$ have been chosen and that we want the system to switch from $\tilde{\Sigma}_i$ to $\tilde{\Sigma}_j$. The parametrisation in $\tilde{x}$ of both can be used to determine exactly how to transition from one gait to the other. In each gait one point should be considered: The point in $\tilde{\Sigma}_i$ at which the switch is executed and the point in $\tilde{\Sigma}_j$ to switch into. Figure 4 shows example trajectories of $\tilde{\Sigma}_i$ and $\tilde{\Sigma}_j$. Any point $\tilde{x}_i \in \left[0, \tilde{L}_{g,i}\right]$ on one step of $\tilde{\Sigma}_i$ can be associated with any point $\tilde{x}_j \in \left[0, \tilde{L}_{g,j}\right]$ on one step of $\tilde{\Sigma}_j$. A combination of two values $(\tilde{x}_{i,opt}, \tilde{x}_{j,opt})$ should exist that minimises some criterion J. Intuitively, to minimise the required control input for transition, we propose to transition at a point at which both gaits have approximately equal momentum of the hip mass, that is, $\mathbf{p}_i(x_i) \approx \mathbf{p}_j(x_j)$ (Figure 4). However, as m is constant, the velocities $\left(\dot{\tilde{x}}, \dot{\tilde{y}}\right)$ are used. As the forward velocity is only controlled during double-support phase, whereas the vertical position is controlled during both single- and double-support, differences in $\dot{\tilde{x}}$ are penalised differently than in $\dot{\tilde{y}}$. Thus, both terms are included separately. Additionally, we include the hip height $\tilde{y}$, as it would be beneficial to switch at a point at which the trajectories are close together, such that the resulting error h_1 is smaller. We then define $J(\tilde{x}_i, \tilde{x}_j)$ as follows:

$$\begin{aligned} J(\tilde{x}_i, \tilde{x}_j) = \mu_1 \left\| \tilde{y}_j(\tilde{x}_j) - \tilde{y}_i(\tilde{x}_i) \right\| + \\ \mu_2 \left\| \dot{\tilde{x}}_j(\tilde{x}_j) - \dot{\tilde{x}}_i(\tilde{x}_i) \right\| + \\ \mu_3 \left\| \dot{\tilde{y}}_j(\tilde{x}_j) - \dot{\tilde{y}}_i(\tilde{x}_i) \right\| \end{aligned} \tag{17}$$

By choosing the weights $\mu_{1,2,3}$, the different aspects of the gait can be emphasised as to achieve a smooth response. The

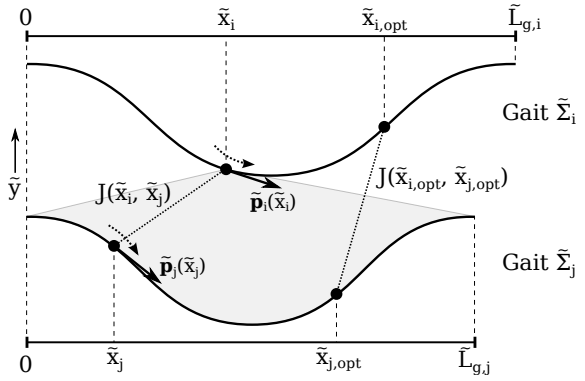

Fig. 4. Optimisation of the switching point from $\tilde{\Sigma}_i$ to $\tilde{\Sigma}_j$. The point $\tilde{x}_i$ is moved along one step of $\tilde{\Sigma}_i$, and $J(\tilde{x}_i, \tilde{x}_j)$ is then calculated for all values of $\tilde{x}_j$ in one step of $\tilde{\Sigma}_j$. Minimisation of J for both these parameters then results in the optimal switching points $(\tilde{x}_{i,opt}, \tilde{x}_{j,opt})$. Note that the gaits shown here are spatially separated, while in practice many gaits will overlap, especially those with equal values of α_0.

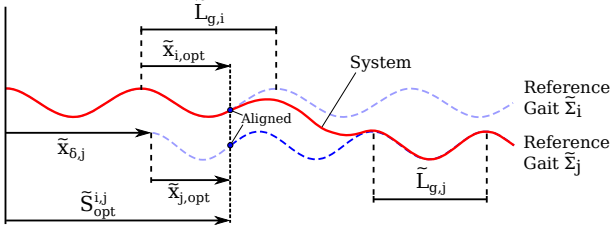

Fig. 5. Aligning optimal points of $\tilde{\Sigma}_i$ and $\tilde{\Sigma}_j$, with step lengths $\tilde{L}_{g,i}$ and $\tilde{L}_{g,j}$ respectively. The trajectory of $\tilde{\Sigma}_j$ is shifted by $\tilde{x}_{\delta,j}$, such that $\tilde{x}_{j,opt}$ aligns with $\tilde{x}_{i,opt}$ at the optimal switching distance $\tilde{S}^{i,j}_{opt}$. The dashed blue lines indicate the natural gait references, the red line indicates an example system response.

criterion J is then minimised numerically with respect to $\tilde{x}_i$ and $\tilde{x}_j$ to obtain the optimal switching points:

$$\min_{\tilde{x}_i, \tilde{x}_j} J(\tilde{x}_i, \tilde{x}_j) \rightarrow (\tilde{x}_{i,opt}, \tilde{x}_{j,opt}) \tag{18}$$

Note that multiple minima may exist, so we search for the global minimum. Due to the use of normalised variables the results are again identical for the same natural gaits on different SLIP systems, and due to symmetry results obtained for $\tilde{\Sigma}_i \rightarrow \tilde{\Sigma}_j$ are also valid for $\tilde{\Sigma}_j \rightarrow \tilde{\Sigma}_i$.

2) Aligning optimal points: As gaits are parametrised as a function of forward distance $\tilde{x}$, we define the gait transitions in terms of forward distance as well. The switching strategy for a single transition is then summarized as follows. Suppose the system is commanded to switch into gait $\tilde{\Sigma}_j$ at a distance $S^{i,j}_{com}$ [m], normalised as $\tilde{S}^{i,j}_{com} = S^{i,j}_{com}/L_0$. We then calculate the optimal switching distance $\tilde{S}^{i,j}_{opt}$, which is the first occurrence of the point $\tilde{x}_{i,opt}$ after this commanded distance (Fig. 5):

$$\tilde{S}^{i,j}_{opt} = \tilde{S}^{i,j}_{com} - \tilde{S}^{i,j}_{com} (\mathrm{mod} \tilde{L}_{g,i}) + \tilde{x}_{i,opt} \tag{19}$$

If $\tilde{S}^{i,j}_{opt} < \tilde{S}^{i,j}_{com}$, we make sure the switching distance is after the commanded distance by calculating $\tilde{S}^{i,j}_{opt} = \tilde{S}^{i,j}_{opt} + \tilde{L}_{g,i}$, that is, delaying the switch by exactly one step. Once the optimal point in the current gait has been reached, the system

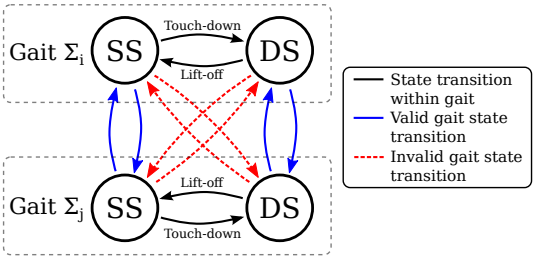

Fig. 6. State transitions during limit cycle walking and gait transition. For a single gait, a transition from single-support to double-support and back occurs every step. When switching gaits in single-support, the system transitions to single-support of the new gait, and vice versa. A transition from double-support of gait $\tilde{\Sigma}_i$ to single-support of gait $\tilde{\Sigma}_j$ (or vice versa) is invalid, as that would require foot lift-off at the moment the controller decides to switch gaits, which is infeasible.

can switch into the new gait by changing α_0, $\tilde{k}$ and the controller references appropriately.

To ensure the system switches from the optimal point in the step of $\tilde{\Sigma}_i$ into the optimal point in the step of $\tilde{\Sigma}_j$, the trajectory of $\tilde{\Sigma}_j$ is shifted in such a way that the point $\tilde{x}_{j,opt}$ aligns with $\tilde{S}^{i,j}_{opt}$ in $\tilde{x}$. The shift $\tilde{x}_{\delta,j}$ of $\tilde{\Sigma}_j$ is calculated as

$$\tilde{x}_{\delta,j} = \tilde{S}^{i,j}_{opt} - \tilde{x}_{j,opt} \tag{20}$$

By shifting the reference of $\tilde{\Sigma}_j$ by $\tilde{x}_{\delta,j}$, the optimal points $(\tilde{x}_{i,opt}, \tilde{x}_{j,opt})$ are aligned in $\tilde{x}$ (Fig. 5).

C. Switching Strategy

At this point we outline the switching strategy. Although the method is general, we make a distinction between switching between gaits with equal values of $(\alpha_0, \tilde{k})$ and gaits with different $(\alpha_0, \tilde{k})$. The first case will be shown to be a special case of the second.

Fig. 6 shows the possible states and transitions for some gaits $\tilde{\Sigma}_i$ and $\tilde{\Sigma}_j$. For a single gait, a transition from single-support to double-support and back occurs every step, at touch-down and lift-off respectively (i.e. when $\tilde{y}$ crosses $\tilde{y}_{td}$). However, if the two gaits have different values of α_0, the current hip height may be defined as double-support in $\tilde{\Sigma}_i$, but as single-support in $\tilde{\Sigma}_j$, i.e. $\tilde{y}_{td,i} > \tilde{y} > \tilde{y}_{td,j}$. This results in an invalid situation if the gait switching is performed instantaneous at that point, as that would require instantaneous foot lift-off at the instant of switching.

However, we do not want to rule out such points entirely by modification of (17). Firstly, because at such points the gait trajectories may be close together in terms of hip height $\tilde{y}$ resulting in smaller error h_1. Secondly, large variations in α_0 may cause gaits to be entirely separated in $\tilde{y}$, such as in Fig. 4, where the entire gait $\tilde{\Sigma}_j$ lies under the touch-down height of $\tilde{\Sigma}_i$. Therefore, for gaits with equal values of $(\alpha_0, \tilde{k})$ instantaneous switching is used, and for gaits with different $(\alpha_0, \tilde{k})$ gait interpolation is used, as outlined below.

1) Instantaneous Switching: As the values of $(\alpha_0, \tilde{k})$ remain constant, we need only to define the controller references $\left(\tilde{y}^*(\tilde{x}), \dot{\tilde{x}}^*(\tilde{x})\right)$ as:

$$\begin{aligned} \tilde{y}^*(\tilde{x}) &= \begin{cases} \tilde{y}_i(\tilde{x}) & \tilde{x} < \tilde{S}^{i,j}_{opt} \\ \tilde{y}_j(\tilde{x} - \tilde{x}_{\delta,j}) & \tilde{x} \geq \tilde{S}^{i,j}_{opt} \end{cases} \\ \dot{\tilde{x}}^*(\tilde{x}) &= \begin{cases} \dot{\tilde{x}}_i(\tilde{x}) & \tilde{x} < \tilde{S}^{i,j}_{opt} \\ \dot{\tilde{x}}_j(\tilde{x} - \tilde{x}_{\delta,j}) & \tilde{x} \geq \tilde{S}^{i,j}_{opt} \end{cases} \end{aligned} \tag{21}$$

2) Gait Interpolation: To avoid invalid gait transitions (Fig. 6) caused by instantaneously changing the value of α_0, we need to ensure the value of α_0 is continuous in $\tilde{x}$. This way we avoid the invalid state transitions in Fig. 6. We extend (21) with a transition period, during which the two gait references are interpolated, together with the corresponding values of α_0 and $\tilde{k}$:

$$\begin{aligned} \tilde{y}^*(\tilde{x}) &= \begin{cases} \tilde{y}_i(\tilde{x}) & \beta \leq 0 \\ (1-\beta)\tilde{y}_i(\tilde{x}) + \beta\tilde{y}_j(\tilde{x} - \tilde{x}_{\delta,j}) & 0 < \beta < 1 \\ \tilde{y}_j(\tilde{x} - \tilde{x}_{\delta,j}) & \beta \geq 1 \end{cases} \\ \dot{\tilde{x}}^*(\tilde{x}) &= \begin{cases} \dot{\tilde{x}}_i(\tilde{x}) & \beta \leq 0 \\ (1-\beta)\dot{\tilde{x}}_i(\tilde{x}) + \beta\dot{\tilde{x}}_j(\tilde{x} - \tilde{x}_{\delta,j}) & 0 < \beta < 1 \\ \dot{\tilde{x}}_j(\tilde{x}) & \beta \geq 1 \end{cases} \\ \alpha_0 &= \begin{cases} \alpha_{0,i} & \beta \leq 0 \\ (1-\beta)\alpha_{0,i} + \beta\alpha_{0,j} & 0 < \beta < 1 \\ \alpha_{0,j} & \beta \geq 1 \end{cases} \\ \tilde{k} &= \begin{cases} \tilde{k}_i & \beta \leq 0 \\ (1-\beta)\tilde{k}_i + \beta\tilde{k}_j & 0 < \beta < 1 \\ \tilde{k}_j & \beta \geq 1 \end{cases} \end{aligned} \tag{22}$$

where the interpolation factor β is defined as $\beta = (\tilde{x} - \tilde{S}^{i,j}_{opt})/\gamma$. The parameter $\gamma \geq 0$ is the transition length. By the definition of the normalised variables, γ effectively is the number of leg lengths in x to interpolate for. Of course, $\left(\tilde{y}^*, \dot{\tilde{x}}^*\right)$ in (22) converge to (21) as $\gamma \to 0$. The reason we use (21) for constant $(\alpha_0, \tilde{k})$ is that then we let the controller handle the transition as quickly as it can, instead of forcing a transition period of fixed length.

V. RESULTS

To demonstrate the effectiveness of the method for large forward velocity differences, first achievable velocity ranges for selected values of $(\alpha_0, \tilde{k})$ that result in symmetric natural gaits is analysed. Simulations were performed in Mathworks MATLAB R2012b, using the ode45 solver with absolute and relative tolerances of 1e-10. The velocity ranges were found by fixing the vertical velocity at VLO to zero, thus enforcing symmetrical gaits [4], and incrementing the forward velocity at VLO in small steps. The resulting velocity ranges are shown in Table I, where $\dot{\tilde{x}}_{avg}$ denotes the normalised average forward velocity and $\dot{x}_{avg}$ denotes the average forward velocity in [m s^{-1}].

Two simulations are performed. In both cases, $m = 80$ kg and $L_0 = 1$ m. Furthermore, $\{\mu_1, \mu_2, \mu_3\} = \{15, 2, 5\}$. In the first simulation (Section V-A), a constant value $(\alpha_0, \tilde{k}) = (70, 20)$ is chosen, and two gaits are selected: a slow gait with average velocity of 0.238 (0.745 m s^{-1}, using (8)) and a fast gait with average velocity 0.372 (1.164 m s^{-1}), an increase of about 56%. Switching between these two gaits corresponds

$(\alpha_0, \tilde{k})$	$\dot{\tilde{x}}_{avg}$ []	$\dot{x}_{avg}$ [m s^{-1}]
$(60, 8)$	0.239–0.344	0.750–1.079
$(62, 10)$	0.236–0.364	0.739–1.140
$(64, 11)$	0.229–0.361	0.719–1.132
$(66, 14)$	0.233–0.379	0.730–1.187
$(68, 16)$	0.229–0.378	0.718–1.183
$(70, 20)$	0.219–0.387	0.687–1.211
$(72, 23)$	0.226–0.380	0.706–1.189

TABLE I

STABLE FORWARD VELOCITY RANGES FOR SYMMETRICAL GAITS WITH SELECTED VALUES OF $(\alpha_0, \tilde{k})$.

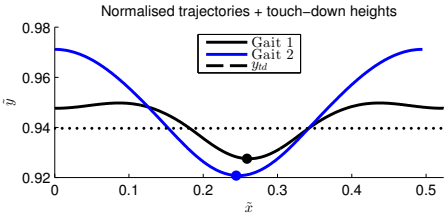

Fig. 7. Hip trajectories for a single step of two gaits with $(\alpha_0, \tilde{k}) = (70, 20)$. The slow gait (1) is double-humped, whereas the faster gait (2) is single-humped. The dotted line `y_td` denotes the touch-down height, and the solid dots denote the optimal points $(\tilde{x}_{1,opt}, \tilde{x}_{2,opt})$.

to moving up and down on one of the vertical bars in Fig. 3, and we use the instantaneous switching method (Section IV-C.1).

In the second (Section V-B), a slow gait with an average velocity of 0.232 (0.725 m s^{-1}) and $(\alpha_0, \tilde{k}) = (64, 11)$ and a fast gait with an average velocity of 0.372 (1.164 m s^{-1}) and $(\alpha_0, \tilde{k}) = (70, 20)$ are chosen, to demonstrate robustness against changing the angle of attack. This corresponds to switching from one point on a vertical bar to another point on another bar in Fig. 3. Here we use the gait interpolation with $\gamma = 1.0$ (Section IV-C.2).

In both cases, the system starts in the slow gait (gait 1), commanded to change to fast gait (gait 2) at 1.0 m, and then switch back to the slow gait (gait 3 = gait 1) at 5.5 m.

A. *Constant* $(\alpha_0, \tilde{k})$

Fig. 7 shows the hip trajectory for a single step of both gaits. The first, i.e. slow gait, is double-humped, whereas the faster gait is single-humped. This likely results from the fact that the natural frequency of the hip mass and leg springs remains approximately constant, while the gait period changes. Calculating J for these two gaits results in $(\tilde{x}_{1,opt}, \tilde{x}_{2,opt}) = (0.259, 0.244)$, which corresponds approximately to the lowest point in both gaits. Of course, for the switch back to the first gait we can use the same values but interchanged. The found values result in optimal switching distances $\tilde{S}^{1,2}_{opt} = 1.306$ and $\tilde{S}^{2,3}_{opt} = 5.762$ respectively (Eq. (19)).

Fig. 8 shows the resulting hip trajectory with the desired and optimal switching points indicated. The hip returns to a periodic trajectory very quickly. Fig. 9 shows the resulting hip height and forward velocity in time, as well as the natural gait references. It can be seen that because the hip

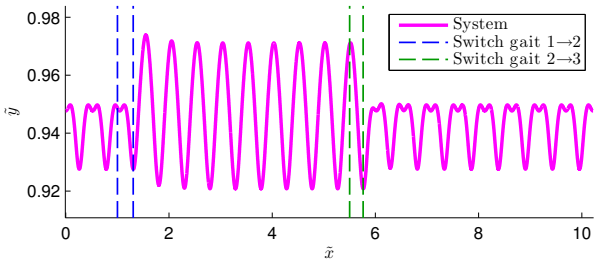

Fig. 8. Hip trajectory for the transition from slow to fast gait and back for two gaits with constant $(\alpha_0, \tilde{k})$. For each pair of vertical dashed lines, the first indicates the commanded switching distance, and the second indicates the resulting optimal switching distance.

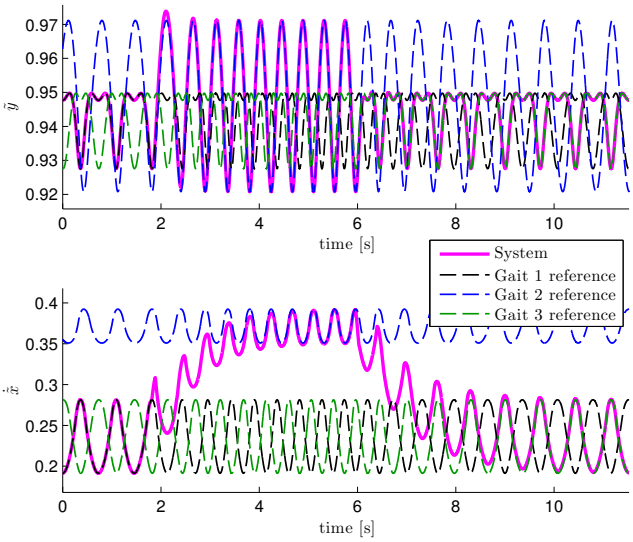

Fig. 9. Hip height and forward velocity over time. The vertical hip motion converges to the new reference within one step. The forward velocity converges in approximately 5 steps.

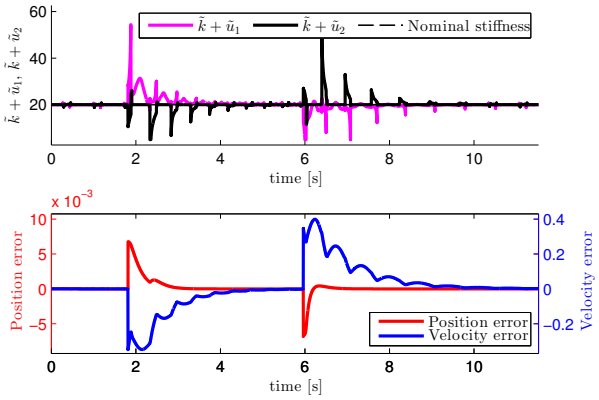

Fig. 10. Control input and error functions. The disturbances that arise from the new references are rejected, after which the leg stiffnesses converge back to their nominal values.

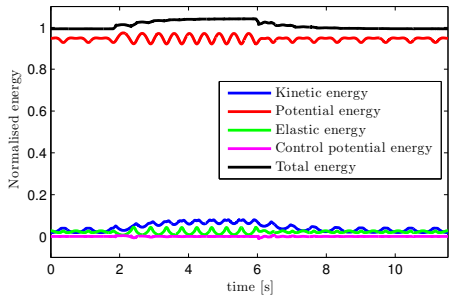

Fig. 11. Energy balance. Most of the increase in total energy is used in the kinetic energy of the system. Some of the additional energy results increased vertical motion of the hip.

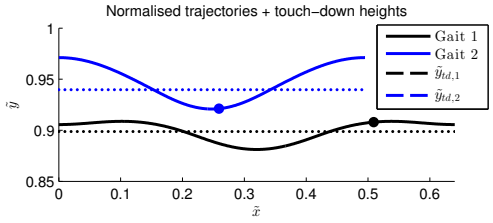

Fig. 12. Hip trajectories for a single step of two gaits with $(\alpha_0, \tilde{k}) = (64, 11)$ and $(70, 20)$ respectively. In contrast with Fig. 7, the gaits are completely separated in $\tilde{y}$ and have different touch-down heights $y_{td,i}$. The solid dots denote the optimal points $(\tilde{x}_{1,opt}, \tilde{x}_{2,opt})$.

height is controlled during both single- and double-support, $\tilde{y}$ converges to the new reference within a single step. The forward velocity $\dot{\tilde{x}}$ converges to the new reference within approximately 5 steps in both transitions. Fig. 10 shows the control inputs and position and velocity errors. The disturbance that arises from the new references is rejected in approximately one second for the hip height and four seconds for the forward velocity respectively, after which the leg stiffnesses converge back to the nominal value. Fig. 11 shows the energy balance. The energy increases from $\tilde{H}_1 = 0.993$ to $\tilde{H}_2 = 1.041$ after the first switch, which if all converted to forward kinetic energy would result in a forward velocity of $\dot{\tilde{x}}_{avg} = 0.388$ (1.216 m s^{-1}). This shows that not all added energy is converted into forward momentum but instead into a vertical motion (Fig. 7) and a minor increase in average hip height.

Remark: The small periodic deviations in the inputs (Fig. 10) after convergence arise due to difference between the approximated gait references using Fourier series and the SLIP model dynamics.

B. Gaits with different $(\alpha_0, \tilde{k})$

Fig. 12 shows the hip trajectory for a single step of both gaits. It can be seen that due to the different values of α_0 the gaits are completely separated in hip height during the entire step; this also results in a significantly smaller step length for the higher gait. Again calculating J for these two gaits, we find $(\tilde{x}_{1,opt}, \tilde{x}_{2,opt}) = (0.509, 0.259)$. This corresponds to approximately the highest point in the first gait and the lowest point in the second gait, arising from the separation of both gaits in terms of hip height. The found values result in

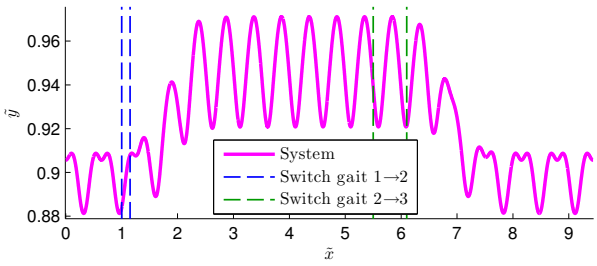

Fig. 13. Hip trajectory for the transition from slow to fast gait and back for two gaits with different $(\alpha_0, \tilde{k})$. For each pair of vertical dashed lines, the first indicates the commanded switching distance, and the second indicates the resulting optimal switching distance.

optimal switching distances $\tilde{S}^{1,2}_{opt} = 1.090$ and $\tilde{S}^{2,3}_{opt} = 6.041$ respectively.

Fig. 13 shows the resulting hip trajectory with the desired and optimal switching points indicated. The trajectory smoothly rises to the new hip height as its shape transforms into that of the second gait. Inspecting the hip height and forward velocity over time (Fig. 14), we see a similar image. The hip oscillation frequency increases as α_0 and forward velocity increase. Note how the forward velocity suddenly increases as the system transitions back to the first gait. This is due to α_0 decreasing, thus lowering touch-down height, leaving more time for the hip mass to accelerate before touch-down. Fig. 15 shows the corresponding control input and error functions. On a few occasions, the leg stiffness reaches the lower limit. After transition, the leg stiffnesses converge to the new gait's nominal $\tilde{k}$ value. Note that during single-support, the stiffness of the swing leg is always equal to $\tilde{k}$ (Eq. (22)), as $\tilde{u}_2 \equiv 0$ in that case (Eq. (14)). The total energy again increases to accommodate the faster gait. The increase is converted in both kinetic and potential energy, while the average elastic energy decreases. The latter can be attributed to the higher, more stiff-legged walk of the second gait.

VI. CONCLUSIONS & FUTURE WORK

A method was presented that allows to switch between natural gaits by actively controlling the leg stiffness. Using this method it is possible to vary the forward velocity during walking by choosing appropriate natural gaits.

First, a normalised notation of natural gaits was introduced. Next a control strategy was proposed that aligns two chosen gaits by minimisation of a criterion, designed such that the transition between the two results in minimal control input. The switch was performed in one of two possible ways; Instantaneous switching for gaits with equal values of the angle of attack and leg stiffness, and gait interpolation with gaits with different values.

It was shown that in both cases the system can be controlled from gait to gait within approximately 5 steps. In both cases, the hip trajectory converges within two steps, but the forward velocity takes longer to converge. After the transition, control action converges to zero as the system converges into limit cycle walking.

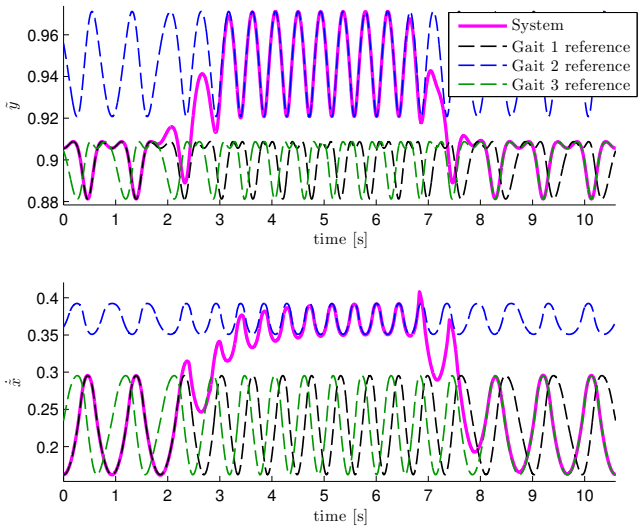

Fig. 14. Hip height and forward velocity over time. The vertical hip motion and forward velocity converge to the new gait in approximately 3 steps.

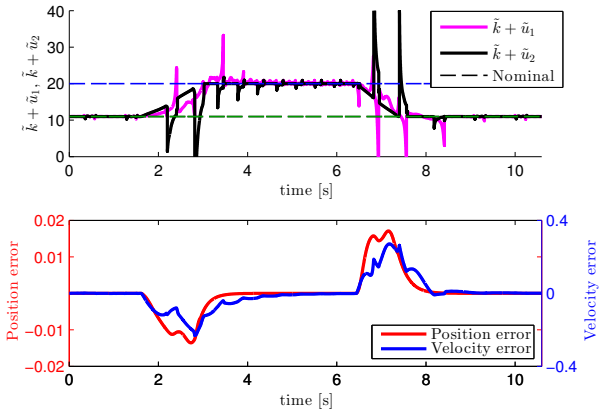

Fig. 15. Control input and error functions. The disturbances that arise from the new references are rejected, after which the leg stiffness converges to a constant value. Note that during single-support, the stiffness of the swing leg is always equal to $\tilde{k}$, as $\tilde{u}_2 \equiv 0$ in that case (Eq. (14)).

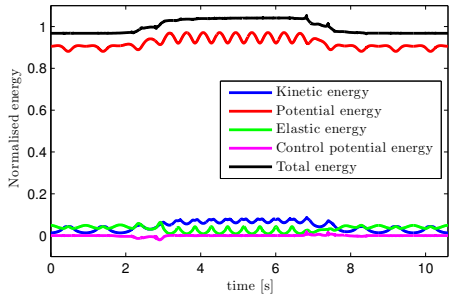

Fig. 16. Energy balance. In the first gait, there is relatively much energy stored as elastic energy, due to the lower leg stiffness. Compared to Fig. 11, there is a significant rise in the potential energy due to the increased hip height of the second gait.

Future work should focus on analysing the robustness of the system during gait transition. Furthermore, it could include a study on more realistic models, such as those including knees and feet, or non-zero leg mass.

REFERENCES

[1] T. McGeer, "Passive dynamic walking," *The International Journal of Robotics Research*, vol. 9, no. 2, pp. 62–82, 1990.

[2] S. Collins and A. Ruina, "A bipedal walking robot with efficient and human-like gait," *Robotics and Automation (ICRA), 2005 IEEE International Conference on*, 2005.

[3] H. Geyer, A. Seyfarth, and R. Blickhan, "Compliant leg behaviour explains basic dynamics of walking and running," in *Proceedings. Biological sciences / The Royal Society*, vol. 273, no. 1603, pp. 2861–7, 2006.

[4] J. Rummel, Y. Blum, and A. Seyfarth, "Robust and efficient walking with spring-like legs," *Bioinspiration & Biomimetics*, vol. 5, no. 4, p. 16, 2010.

[5] L. C. Visser, S. Stramigioli, and R. Carloni, "Robust Bipedal Walking with Variable Leg Stiffness," in *Proceedings of the 2012 4th IEEE RAS & EMBS International Conference on Biomedical Robotics and Biomechatronics (BioRob)*, pp. 1626–1631, 2012.

[6] H. R. Martinez Salazar and J. P. Carbajal, "Exploiting the passive dynamics of a compliant leg to develop gait transitions," *Physical Review E*, vol. 83, no. 6, p. 066707, 2011.

[7] T. Haarnoja, J.-L. Peralta-Cabezas, and A. Halme, "Model-based velocity control for Limit Cycle Walking," *2011 IEEE/RSJ International Conference on Intelligent Robots and Systems*, pp. 2255–2260, 2011.

[8] Y. Huang, B. Vanderborght, R. Van Ham, Q. Wang, M. Van Damme, G. Xie, and D. Lefeber, "Step Length and Velocity Control of a Dynamic Bipedal Walking Robot With Adaptable Compliant Joints," *IEEE/ASME Transactions on Mechatronics*, vol. 18, no. 2, pp. 598–611, 2013.

[9] D. G. E. Hobbelen and M. Wisse, "Controlling the Walking Speed in Limit Cycle Walking," *The International Journal of Robotics Research*, vol. 27, no. 9, pp. 989–1005, 2008.

[10] S. V. Kuznetsov, "The motion of the elastic pendulum," *Regular and Chaotic Dynamics*, vol. 4, no. 3, pp. 3–12, 1999.

3 Paper 2: Bipedal Walking Gait with Segmented Legs and Variable Stiffness Knees

Will be submitted to BIOROB 2014.

Abstract – This work investigates the control of bipedal walking robots based on the principle of passive dynamic walking. We propose the Segmented Spring-Loaded Inverted Pendulum (S-SLIP) model, and show that it exhibits walking gait and can be controlled from one limit cycle walking gait to another using control of the knee stiffness. Furthermore, based on the S-SLIP model, a realistic bipedal robot model is designed that uses Variable Stiffness Actuators (VSAs) to control the knees and thus leg stiffness. The variable leg stiffness is then to stabilise the system into a walking gait and to inject energy losses generated by friction and foot impacts. It is shown that this results in a stable limit cycle walking gait.

Bipedal Walking Gait with Segmented Legs and Variable Stiffness Knees

W. Roozing and R. Carloni

***Abstract*— We use the Segmented Spring-Loaded Inverted Pendulum (S-SLIP) model, and show that it exhibits walking gait. We propose a control architecture that can control the system from one limit cycle walking gait to another using control of the knee stiffness. Furthermore, based on the S-SLIP model, a realistic bipedal robot model is designed that uses Variable Stiffness Actuators (VSAs) to control the knees and thus leg stiffness. The variable leg stiffness is then to stabilise the system into a walking gait and to inject energy losses generated by friction and foot impacts. It is shown that this results in a stable limit cycle walking gait.**

I. INTRODUCTION

The high performance of human walking, which combines high robustness with high energy efficiency, has long been the inspiration of efforts to design robots based on the principle of passive dynamic walking. In contrast, most existing systems are either energy efficient or robust. Robots based on the principle of passive dynamic walking show high energy efficiency, but are not robust against external disturbances [1]. Highly controlled systems – often based on the concept of Zero Moment Point (ZMP) – are robust at the exchange of energy efficiency [2].

It has been shown that humans walking on flat terrain can be accurately modeled using inverted spring-mass systems. The Spring-Loaded Inverted Pendulum (SLIP) has been shown to exhibit autonomous stable limit cycle walking gait [4] strongly comparable to human walking in terms of hip trajectory, single- and double-support phases and ground contact forces [3].

In this work we propose a control strategy for the Segmented Spring-Loaded Inverted Pendulum (S-SLIP) model, which is different from the SLIP model in that it has segmented legs with torsional stiffness knees, which is more realistic when compared with existing robot designs, which use knees and leg retraction to avoid food scuffing. For the S-SLIP model, the foot-hip stiffness is nonlinear, arising from the two-link leg geometry. It has been shown that given proper initial conditions, the uncontrolled S-SLIP model exhibits autonomous stable limit cycle running gait [5]. However, the model also shows passive limit cycle walking gait similar to the SLIP model. Fig. 1 shows an S-SLIP walking gait, compared to a SLIP walking gait at an average forward velocity of 1.00 m s^{-1}. Both systems have equal mass and leg lengths of $\approx$ 1.0 m. While the hip trajectories are similar, there is a clear difference in forward velocity profiles.

W. Roozing and R. Carloni are with the Robotics And Mechatronics group, MIRA Institute, University of Twente, The Netherlands. E-mail: w.roozing@student.utwente.nl, r.carloni@utwente.nl

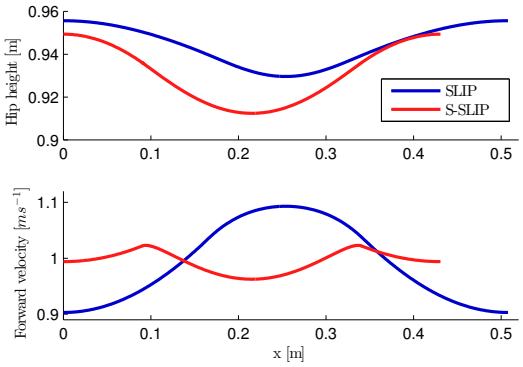

Fig. 1. SLIP vs S-SLIP walking gaits at average velocities of 1.00 m s^{-1}. Both systems have equal mass and leg lengths of $\approx$ 1.0 m. While the trajectories are comparable, there is a difference in forward velocity profile due to high stiffness of the segmented leg just after impact.

The segmented leg has high stiffness just after impact due to its configuration, which quickly decreases as the leg is compressed. The result is that the forward velocity is reduced during double support when compared to the linear leg of the SLIP model.

The control strategy developed in this work uses variable leg stiffness to stabilise the system after a disturbance and from one limit cycle walking gait to another. The performance of this strategy is shown by a simulated controlled S-SLIP system that switches between two gaits with a large forward velocity difference.

Furthermore, a realistic bipedal robot model is designed that uses Variable Stiffness Actuators (VSAs) to control the knees and thus leg stiffness. The control is based on the developed strategy for the S-SLIP model, and is extended with additional components to facilitate leg swing and leg retraction, which arise due to the additional dynamics of this model. A reference gait is obtained by using this model with constant leg stiffness. The variable leg stiffness is then used to stabilise the system into this gait and to inject energy losses generated by foot impacts. It is shown that this results in a stable limit cycle walking gait.

The remainder of this paper is outlined as follows. Section II describes the S-SLIP model and its dynamics. The proposed control design for the S-SLIP model is described in Section III, followed by simulation results in Section IV. The bipedal robot model is presented in Section V, its control in Section VI, followed by simulation results in Section VII. The paper concludes with conclusions and recommendations for future work in Section VIII.

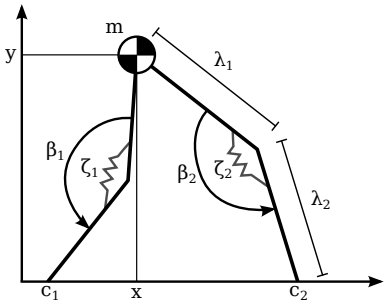

Fig. 2. The S-SLIP model consists of a hip point mass, with two massless segmented legs with links of length λ_1 and λ_2. In the knees with angles β_1 and β_2 there are torsional springs with stiffnesses ζ_1 and ζ_2. The legs touch the ground at the foot contact points c_1 and c_2.

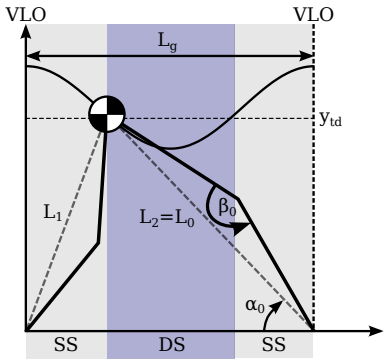

Fig. 3. A single step of the S-SLIP model, shown at touch-down. The leg that has just touched down is at its rest length L_0 and rest knee angle β_0, and the virtual leg from hip mass to foot contact (dashed line) is at an angle α_0 with the ground. The step starts and ends at VLO and has length L_g. The virtual leg lengths are defined as L_1 and L_2. At touch-down, the system transitions to double-support (DS) phase, during which both legs are in contact with the ground. The transition back to single-support (SS) occurs when the trailing virtual leg L_1 reaches its rest length. Touch-down and lift-off occur when the hip mass crosses the touch-down height y_{td}.

II. Segmented Spring-Loaded Inverted Pendulum (S-SLIP)

In this Section the S-SLIP model is described. We describe the configuration manifold and conditions for state transition. Next the system dynamics are derived and we conclude with a S-SLIP limit cycle gaits and a normalised description.

A. Configuration Manifold & State Transitions

The Segmented Spring-Loaded Inverted Pendulum (S-SLIP) model is shown in Fig. 2. It consists of a hip point mass m, connected to two massless segmented legs, each composed of two links with upper leg length λ_1 and lower leg length λ_2. Between the links there are torsional springs with stiffnesses ζ_1 and ζ_2, and the knee angles are defined as β_1 and β_2. The foot contact points are denoted by c_1 and c_2.

The configuration of the system is given by the position of the hip mass as $(x, y) =: \mathbf{q} \in \mathcal{Q}$, and its velocity by $\dot{\mathbf{q}} \in T_{\mathbf{q}}\mathcal{Q}$, the tangent space to $\mathcal{Q}$ at $\mathbf{q}$. The system state is then given as $\mathbf{x} := (\mathbf{q}, \mathbf{p})$, with the momentum $\mathbf{p} := (p_x, p_y) = M\dot{\mathbf{q}}$ and the mass matrix $M = \mathrm{diag}(m, m)$.

As in [4] and [6], a single step is defined as a trajectory $\mathbf{q}(t) \in \mathcal{Q}$ that starts with the system in Vertical Leg Orientation (VLO), where the hip mass is exactly above the supporting leg. The step ends when the system again reaches VLO (Fig. 3), and the role of the legs is then exchanged. We define the gait length $L_g := x(T)$, where T is the gait time period, i.e. $\mathbf{q}(t) = \mathbf{q}(t + T)$ after which a new step starts.

Every step consists of two distinct phases, i.e. single-support (SS) and double-support (DS) during which either one or two legs are in contact with the ground, respectively. The SS→DS transition occurs when the swing leg touches down, when the length is equal to the rest length L_0, that is, the length of the leg when the knee is at its rest angle β_0:

$$L_0 = \sqrt{\lambda_1^2 + \lambda_2^2 - 2\lambda_1\lambda_2 \cos(\beta_0)} \tag{1}$$

At this moment the hip mass is at the touch-down height y_{td}, corresponding to the angle-of-attack α_0, i.e. at touch-down the leading leg is at an angle α_0 with the ground so that $y = y_{td} := L_0 \sin(\alpha_0)$. At this moment, the foot contact point is $c_2 = x + L_0 \cos(\alpha_0)$.

Conversely, the DS→SS transition occurs when the trailing leg reaches its rest length. The swing leg disappears, and reappears at the subsequent moment of touch-down, which is possible because the leg is massless. In the nominal case, only the trailing leg reaches its rest length and contact c_2 is relabeled as c_1 to correspond to the notation used during SS phase. During SS, the swing leg knee is at its rest angle, i.e. $\beta_2 \equiv \beta_0$ and the leg exerts no force. We can now define two subsets of $\mathcal{Q}$ which correspond to the single- and double-support phases respectively:

$$\begin{aligned} \mathcal{Q}_{SS} &= \{\mathbf{q} \in \mathcal{Q} \,|\, y > y_{td}\,,\; y < L_0\} \\ \mathcal{Q}_{DS} &= \{\mathbf{q} \in \mathcal{Q} \,|\, y < y_{td}\,,\; y > 0\} \end{aligned} \tag{2}$$

where the conditions $y < L_0$ and $y > 0$ assure to avoid the remaining cases, i.e. lift-off and fall respectively. Note that for a walking gait $\mathbf{q} \in \mathcal{Q}_{SS} \cup \mathcal{Q}_{DS}$.

During contact, the length L_i of each leg is given by

$$L_i = \sqrt{(x - c_i)^2 + y^2}\,, \quad i \in \{1, 2\} \tag{3}$$

with corresponding knee angle β_i

$$\beta_i = \cos^{-1}\left(\frac{\lambda_1^2 + \lambda_2^2 - L_i^2}{2\lambda_1\lambda_2}\right),\; i \in \{1, 2\} \tag{4}$$

Remark: Lift-off is also possible while $\mathbf{q} \in \mathcal{Q}_{SS} \cup \mathcal{Q}_{DS}$. We take care of this in simulation by checking $L_1 \leq L_0 \vee L_2 \leq L_0$, i.e. at least one leg is in contact with the ground.

B. System Dynamics

To derive the dynamic equations for the system, we use the Hamiltonian approach. The kinetic energy function is defined as $K = \frac{1}{2}\mathbf{p}^T M^{-1}\mathbf{p}$ and the potential energy function as

$$V = mgy + \frac{1}{2}\zeta_1 (\beta_0 - \beta_1)^2 + \frac{1}{2}\zeta_2 (\beta_0 - \beta_2)^2$$

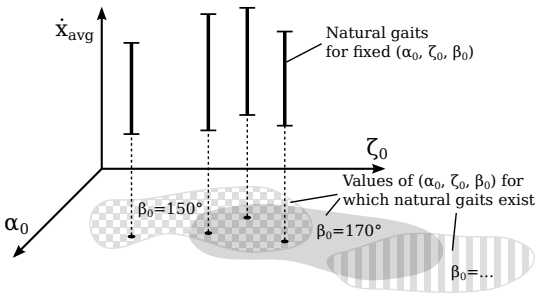

Fig. 4. Average forward velocities $\dot{\mathbf{x}}_{avg}$ of natural gaits for different values of $(\alpha_0, \zeta_0, \beta_0)$. Note that for given $(\alpha_0, \zeta_0, \beta_0)$, the average forward velocity is proportional to the system energy H.

where g is the gravitational acceleration. The dynamic equations are then defined by the Hamiltonian energy function $H = K + V$ as

$$\frac{\mathrm{d}}{\mathrm{d}t}\begin{bmatrix}\mathbf{q}\\ \mathbf{p}\end{bmatrix} = \begin{bmatrix}0 & I\\ -I & 0\end{bmatrix}\begin{bmatrix}\frac{\delta H}{\delta \mathbf{q}}\\ \frac{\delta H}{\delta \mathbf{p}}\end{bmatrix} \tag{5}$$

Note that a solution $\mathbf{q}(t)$ of (5) is of class C^2, due to the non-differentiability of the leg forces at the moment of transition between the single- and double-support phases.

C. S-SLIP Limit Cycle Gaits

A limit cycle gait is a periodic walking gait, which returns to the same state periodically. From this point on, we refer to limit cycle walking gaits of the S-SLIP model as *natural gaits*.

In the description of natural gaits, we use the state at VLO as initial conditions, i.e. $\mathbf{x}_0 = (\mathbf{q}, \mathbf{p})_0 = (x, y, p_x, p_y)_0$, and, during walking in natural gait, the system returns to this state at every VLO. Since we can take at every VLO $x \equiv 0$, a natural gait can then be fully described as

$$\Sigma = (\alpha_0, \zeta_0, L_0, m, \beta_0, y_0, p_{x,0}, p_{y,0}) \tag{6}$$

where ζ_0 is the nominal knee stiffness and $\zeta_1 = \zeta_2 = \zeta_0$. Note that it is not possible to use the total system energy H to uniquely describe a natural gait, because energy can be stored in either potential (leg compression, hip height) or kinetic (hip momentum) energy. As natural gaits exist for ranges of parameters, there often exists a range of natural gaits that achieve a desired forward velocity (Fig. 4). Conversely, a single set $(\alpha_0, \zeta_0, \beta_0)$ can often achieve a range of average forward velocities (vertical bar in Fig. 4).

D. Normalised Notation of S-SLIP Limit Cycle Gaits

The torsional knee stiffness ζ_0 and energy H can be normalised in dimensionless form as

$$\tilde{\zeta} = \frac{\zeta_0}{mgL_0} \qquad \tilde{H} = \frac{H}{mgL_0} \tag{7}$$

If we normalise $\mathbf{x}$ as $\tilde{\mathbf{x}} := (\tilde{\mathbf{q}}, \tilde{\mathbf{p}}) = (\tilde{x}, \tilde{y}, \tilde{p}_x, \tilde{p}_y)$ with

$$\tilde{x} = \frac{x}{L_0} \quad \tilde{y} = \frac{y}{L_0} \quad \tilde{p}_x = \frac{p_x}{m\sqrt{L_0 g}} \quad \tilde{p}_y = \frac{p_y}{m\sqrt{L_0 g}} \tag{8}$$

and use (7), we obtain a fully normalised unique description $\tilde{\Sigma}$ of a natural gait:

$$\tilde{\Sigma} = \left(\alpha_0, \tilde{\zeta}, \beta_0, \tilde{y}_0, \tilde{p}_{x,0}, \tilde{p}_{y,0}\right) \tag{9}$$

The gait trajectory can then be found by solving (5) for $\tilde{\Sigma}$. Using this description, equal gaits on different S-SLIP systems now result in the same normalised state trajectory $\tilde{\mathbf{x}}(t) = (\tilde{\mathbf{q}}(t), \tilde{\mathbf{p}}(t))$. Similarly to $\tilde{p}_x, \tilde{p}_y$, the velocities are normalised as

$$\dot{\tilde{x}} = \frac{\dot{x}}{\sqrt{L_0 g}} \qquad \dot{\tilde{y}} = \frac{\dot{y}}{\sqrt{L_0 g}} \tag{10}$$

Note that the normalisation $\dot{\tilde{x}}$ is the Froude number Fr [9], [10], used to compare the relative walking speeds of systems with different leg lengths.

III. S-SLIP CONTROL DESIGN

The control design of the controlled S-SLIP model is inspired by [6]. By actively controlling the leg stiffness of the legs, the rejection of external disturbances to the system can be significantly increased. Furthermore, after a disturbance, the system can be stabilised into its original gait by injecting or removing energy appropriately.

The knee stiffnesses are defined as $\zeta_i = \zeta_0 + u_i, i \in \{1, 2\}$ (Fig. 2) with the control inputs u_i restricted to subsets $U_i = \{u_i \in \mathbb{R} \mid 0 < \zeta_0 + u_i < \infty\}$, such that the result is a meaningful stiffness value. We intend to control the system towards a reference gait $\tilde{\Sigma}$ with normalised state trajectory $\tilde{\mathbf{x}}(t)$, i.e. to a reference state trajectory $\tilde{\mathbf{x}}^o(t)$ such that $u_i \to 0, i \in \{1, 2\}$. However, during single-support phase the system has only one control input and $\tilde{\mathbf{x}}^o(t)$ cannot be tracked exactly, which may lead to instability as the system lags behind the reference. As $\tilde{x}$ was identified to be a periodic variable and required to be monotonically increasing in time, the references are reparametrised on $\tilde{x}$. The references $\tilde{y}^*(\tilde{x}), \dot{\tilde{x}}^*(\tilde{x})$ are then sufficiently described as

$$\tilde{y}^*(\tilde{x}) = \tilde{y}^o(\tilde{x}) \qquad \dot{\tilde{x}}^*(\tilde{x}) = \dot{\tilde{x}}^o(\tilde{x}) \tag{11}$$

However, as a general analytic expression for the spring-loaded pendulum does not exist [11], a Fourier series expansion approximation of the numerical solution is used. We extend Eq. (5) to obtain

$$\frac{\mathrm{d}}{\mathrm{d}t}\begin{bmatrix}\mathbf{q}\\ \mathbf{p}\end{bmatrix} = \begin{bmatrix}0 & I\\ -I & 0\end{bmatrix}\begin{bmatrix}\frac{\delta H}{\delta \mathbf{q}}\\ \frac{\delta H}{\delta \mathbf{p}}\end{bmatrix} + \begin{bmatrix}0\\ B\end{bmatrix}\mathbf{u} \tag{12}$$

with $\mathbf{u} = [u_1, u_2]$ the controlled part of the leg stiffness. The input matrix B is given by

$$B = \begin{bmatrix}\frac{\mathrm{d}\phi_1}{\mathrm{d}x} & \frac{\mathrm{d}\phi_2}{\mathrm{d}x}\\ \frac{\mathrm{d}\phi_1}{\mathrm{d}y} & \frac{\mathrm{d}\phi_2}{\mathrm{d}y}\end{bmatrix} \tag{13}$$

with

$$\phi_i = \frac{1}{2}\left(\beta_0 - \beta_i\right)^2, \quad i \in \{1, 2\} \tag{14}$$

calculated from (3)–(4). To formulate the control strategy, we rewrite Eq. (12) in standard form as

$$\dot{\mathbf{x}} = f(\mathbf{x}) + \sum_i g_i(\mathbf{x}) u_i \tag{15}$$

and then define error functions h_1 and h_2 as

$$\begin{aligned} h_1 &= y - y^* \\ h_2 &= \dot{x} - \dot{x}^* \end{aligned} \tag{16}$$

The control solution is then given as follows.

- For $\mathbf{q} \in \mathcal{Q}_{SS}$ and $|x - c_1| \leq \epsilon$:

$$\begin{aligned} u_1 &= \frac{1}{L_{g_1} L_f h_1} \left(-L_f^2 h_1 - \kappa_d L_f h_1 - \kappa_p h_1 \right) \\ u_2 &\equiv 0 \end{aligned} \tag{17}$$

- For $\mathbf{q} \in \mathcal{Q}_{SS}$ and $|x - c_1| > \epsilon$:

$$\begin{aligned} u_1 &= \frac{1}{L_{g_1} h_2} \left(-L_f h_2 - \kappa_v h_2 \right) \\ u_2 &\equiv 0 \end{aligned} \tag{18}$$

- For $\mathbf{q} \in \mathcal{Q}_{DS}$:

$$\begin{bmatrix} u_1 \\ u_2 \end{bmatrix} = A^{-1} \begin{bmatrix} -L_f^2 h_1 - \kappa_d L_f h_1 - \kappa_p h_1 \\ -L_f h_2 - \kappa_v h_2 \end{bmatrix} \tag{19}$$

with

$$A = \begin{bmatrix} L_{g_1} L_f h_1 & L_{g_2} L_f h_1 \\ L_{g_1} L_f h_2 & L_{g_2} L_f h_2 \end{bmatrix} \tag{20}$$

where $L_f^2 h_i$, $L_f h_i$, $L_{g_i} h_i$ and $L_{g_i} L_f h_i$ denote the (repeated) Lie-derivatives of h_i along the vector fields defined in (15), $\kappa_d, \kappa_p, \kappa_v$ are tunable control parameters and $\epsilon \in [0, \frac{1}{2} L_g]$ is the distance around VLO during which h_1 should be controlled instead of h_2. The control inputs (17), (18), (19) ensure that the error h_1 converges asymptotically to zero and that the error h_2 is at least bounded [6].

Remark: Due to only one control input being available during single-support phase, the system is not always fully controllable. Because at VLO the velocity error cannot be controlled due to leg orientation, we choose to control the hip height error h_1 around VLO and control the velocity error h_2 just after touch-down and just before lift-off.

A. Gait Switching

1) Finding Optimal Points: Suppose that two natural gaits $\tilde{\Sigma}_i$ and $\tilde{\Sigma}_j$, with step lengths $\tilde{L}_{g,i}, \tilde{L}_{g,j}$ respectively, have been chosen and that we want the system to switch from $\tilde{\Sigma}_i$ to $\tilde{\Sigma}_j$. The parametrisation of both can be used to determine exactly how to transition from one gait to the other. In each gait one point should be considered: The point in $\tilde{\Sigma}_i$ at which the switch is executed and the point in $\tilde{\Sigma}_j$ to switch into. Any point $\tilde{x}_i \in \left[0, \tilde{L}_{g,i}\right)$ on one step of $\tilde{\Sigma}_i$ can be associated with any point $\tilde{x}_j \in \left[0, \tilde{L}_{g,j}\right)$ on one step of $\tilde{\Sigma}_j$. To find this set of points $(\tilde{x}_{i,opt}, \tilde{x}_{j,opt})$, we minimise the criterion $J(\tilde{x}_i, \tilde{x}_j)$ w.r.t. $(\tilde{x}_i, \tilde{x}_j)$:

$$\begin{aligned} J(\tilde{x}_i, \tilde{x}_j) = \mu_1 &\left| \tilde{y}_j(\tilde{x}_j) - \tilde{y}_i(\tilde{x}_i) \right| + \\ \mu_2 &\left| \dot{\tilde{x}}_j(\tilde{x}_j) - \dot{\tilde{x}}_i(\tilde{x}_i) \right| + \\ \mu_3 &\left| \dot{\tilde{y}}_j(\tilde{x}_j) - \dot{\tilde{y}}_i(\tilde{x}_i) \right| \end{aligned} \tag{21}$$

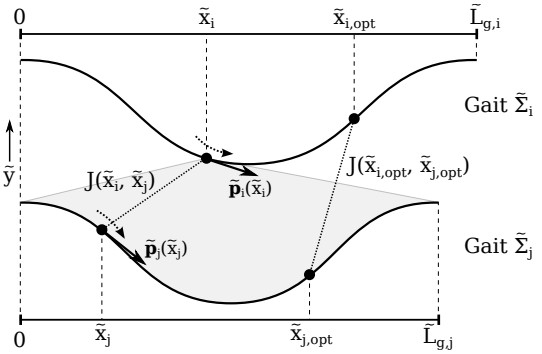

Fig. 5. Optimisation of the switching point from $\tilde{\Sigma}_i$ to $\tilde{\Sigma}_j$. The point $\tilde{x}_i$ is moved along one step of $\tilde{\Sigma}_i$, and $J(\tilde{x}_i, \tilde{x}_j)$ is then calculated for all values of $\tilde{x}_j$ in one step of $\tilde{\Sigma}_j$. Minimisation of J for both these parameters then results in the optimal switching points $(\tilde{x}_{i,opt}, \tilde{x}_{j,opt})$.

By choosing the weights $\{\mu_1, \mu_2, \mu_3\}$, the different aspects of the gait can be emphasised as to achieve a smooth response. Note that multiple minima may exist, so we search for the global minimum. Due to the use of normalised variables the results are again identical for the same natural gaits on different SLIP systems, and due to symmetry results obtained for $\tilde{\Sigma}_i \to \tilde{\Sigma}_j$ are also valid for $\tilde{\Sigma}_j \to \tilde{\Sigma}_i$. In the next sections we outline the switching strategy. Although the method is general, we make a distinction between switching between gaits with equal values of $(\alpha_0, \tilde{\zeta})$ and gaits with different $(\alpha_0, \tilde{\zeta})$. The first case will be shown to be a special case of the second.

2) Instantaneous Switching: In the case in which $(\alpha_0, \tilde{\zeta})$ remain constant, we can switch the references of the S-SLIP controller instantaneously at the desired point, and we need only to redefine the controller references $\left(\tilde{y}^*(\tilde{x}), \dot{\tilde{x}}^*(\tilde{x})\right)$ as:

$$\begin{aligned} \tilde{y}^*(\tilde{x}) &= \begin{cases} \tilde{y}_i(\tilde{x}) & \tilde{x} < \tilde{S}_{opt}^{i,j} \\ \tilde{y}_j(\tilde{x} - \tilde{x}_{\delta,j}) & \tilde{x} \geq \tilde{S}_{opt}^{i,j} \end{cases} \\ \dot{\tilde{x}}^*(\tilde{x}) &= \begin{cases} \dot{\tilde{x}}_i(\tilde{x}) & \tilde{x} < \tilde{S}_{opt}^{i,j} \\ \dot{\tilde{x}}_j(\tilde{x} - \tilde{x}_{\delta,j}) & \tilde{x} \geq \tilde{S}_{opt}^{i,j} \end{cases} \end{aligned} \tag{22}$$

where $\tilde{S}_{opt}^{i,j}$ is the normalised switching distance which coincides with the point $\tilde{x}_i$ on the current gait. The reference of $\tilde{\Sigma}_j$ is shifted by $\tilde{x}_{\delta,j}$ such that the points $(\tilde{x}_{i,opt}, \tilde{x}_{j,opt})$ align at $\tilde{S}_{opt}^{i,j}$.

3) Gait Interpolation: In the case the two gaits have different values of $(\alpha_0, \tilde{\zeta})$, we ensure the value of α_0 is continuous in $\tilde{x}$. We extend (22) with a transition period, during which the two gait references are interpolated, together with

the corresponding values of α_0 and $\tilde{\zeta}$:

$$\tilde{y}^*(\tilde{x}) = \begin{cases} \tilde{y}_i(\tilde{x}) & \beta \leq 0 \\ (1-\beta)\tilde{y}_i(\tilde{x}) + \beta\tilde{y}_j(\tilde{x}-\tilde{x}_{\delta,j}) & 0 < \beta < 1 \\ \tilde{y}_j(\tilde{x}-\tilde{x}_{\delta,j}) & \beta \geq 1 \end{cases}$$

$$\dot{\tilde{x}}^*(\tilde{x}) = \begin{cases} \dot{\tilde{x}}_i(\tilde{x}) & \beta \leq 0 \\ (1-\beta)\dot{\tilde{x}}_i(\tilde{x}) + \beta\dot{\tilde{x}}_j(\tilde{x}-\tilde{x}_{\delta,j}) & 0 < \beta < 1 \\ \dot{\tilde{x}}_j(\tilde{x}) & \beta \geq 1 \end{cases}$$

$$\alpha_0 = \begin{cases} \alpha_{0,i} & \beta \leq 0 \\ (1-\beta)\alpha_{0,i} + \beta\alpha_{0,j} & 0 < \beta < 1 \\ \alpha_{0,j} & \beta \geq 1 \end{cases}$$

$$\tilde{\zeta} = \begin{cases} \tilde{\zeta}_i & \beta \leq 0 \\ (1-\beta)\tilde{\zeta}_i + \beta\tilde{\zeta}_j & 0 < \beta < 1 \\ \tilde{\zeta}_j & \beta \geq 1 \end{cases} \quad (23)$$

where the interpolation factor β is defined as $\beta = (\tilde{x} - \tilde{S}^{i,j}_{opt})/\gamma$. The parameter $\gamma \geq 0$ is the transition length. By the definition of the normalised variables, γ effectively is the number of leg lengths in x to interpolate for. Of course, $(\tilde{y}^*, \dot{\tilde{x}}^*)$ in (23) converge to (22) as $\gamma \to 0$. The reason we use (22) for constant $(\alpha_0, \tilde{\zeta})$ is that then we let the controller handle the transition as quickly as it can, instead of forcing a transition period of fixed length.

IV. S-SLIP SIMULATION RESULTS

To demonstrate the effectiveness of the method for forward velocity differences, a slow gait with an average velocity of 0.259 (0.811 m s^{-1}) and $(\alpha_0, \tilde{\zeta}) = (70, 0.224)$ and a fast gait with an average velocity of 0.457 (1.429 m s^{-1}) and $(\alpha_0, \tilde{\zeta}) = (65, 0.224)$ are chosen, to demonstrate robustness against changing the angle of attack. Here we use the gait interpolation with $\gamma = 1.0$ (Sec. III-A.3). Furthermore, $m = 80$ kg, $\lambda_1 = \lambda_2 = 0.50$ m, $\beta_0 = 170$ deg (s.t. $L_0 \approx 0.996$ m), $\{\mu_1, \mu_2, \mu_3\} = \{15, 2, 5\}$ and for the S-SLIP control $\{\epsilon, \kappa_p, \kappa_d, \kappa_v\} = \{0.1, 50, 25, 50\}$. From $\tilde{\zeta} = 0.224$ follows $\zeta_0 \approx 175$ N m rad^{-1} (Eq. (7)). Simulations were performed in Mathworks MATLAB R2012b, using the ode45 solver with absolute and relative tolerances of 1e-11. The velocity ranges were found by fixing the vertical velocity at VLO to zero, thus enforcing symmetrical gaits [4], and incrementing the forward velocity at VLO in small steps. The system starts in the slow gait (gait 1), is commanded to change to fast gait (gait 2) at 1.0 m, and then to switch back to the slow gait (gait 3 = gait 1) at 5.5 m.

Fig. 6 shows the resulting hip trajectory with the desired and optimal switching points indicated. The trajectory smoothly lowers to the new hip height as its shape transforms into that of the second gait. Fig. 7 shows the hip height and forward velocity over time, which converge to the new gait in approximately 5 steps. Fig. 8 shows the corresponding control input and error functions. On a few occasions, the stiffness of the trailing leg reaches the lower limit due to the system attempting to slow down. After transition, the leg stiffnesses converge to the nominal ζ_0 value. Note that during single-support, the stiffness of the swing leg is always equal to ζ_0, as $\tilde{u}_2 \equiv 0$ in that case (Eq. (17)–(18)).

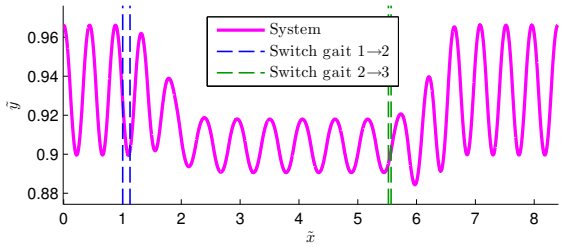

Fig. 6. Hip trajectory for the transition from slow to fast gait and back for two gaits with different $(\alpha_0, \tilde{\zeta})$. For each pair of vertical dashed lines, the first indicates the commanded switching distance, and the second indicates the resulting optimal switching distance.

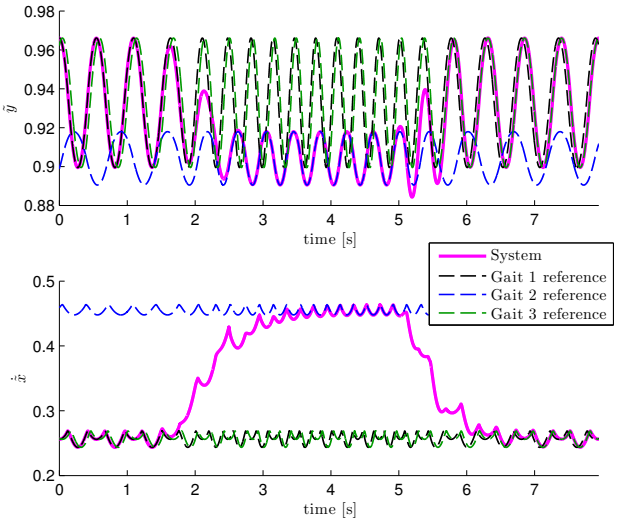

Fig. 7. Hip height and forward velocity over time. The system converges to the new gait in approximately 5 steps.

Fig. 9 shows the energy balance. Most of the total energy increase on transition is put into (forward) kinetic energy, to accommodate the faster gait.

V. BIPEDAL ROBOT MODEL

The bipedal robot model is based on the mechanical design of an existing bipedal walker [7] (Fig. 10). It is a four-link model with segments of length λ_1 and λ_2 similar to the S-SLIP model. However, the hip mass is replaced by two separate upper-leg masses $m_{h,l}, m_{h,r}$ – there is a small mass difference between left and right on the physical robot due to electronics and a guide rail – and two lower-leg masses m_l are added (Fig. 11). The hip joint position is denoted (x, y), similar to the S-SLIP model. In the same way, the knee joint angles are denoted β_l, β_r respectively. Conversely to the S-SLIP model, the swing leg does not disappear during swing, and we denote the angles of attack of the virtual legs α_l, α_r. The angle-of-attack of the virtual stance leg (during SS) or virtual leading leg (during DS) is always denoted as α. The hip angle is denoted θ. There are three control inputs to the system; hip torque τ_h, left knee torque τ_l and right knee torque τ_r. The hip torque is generated by a realistic motor & gearbox dynamics model and the knee torques are

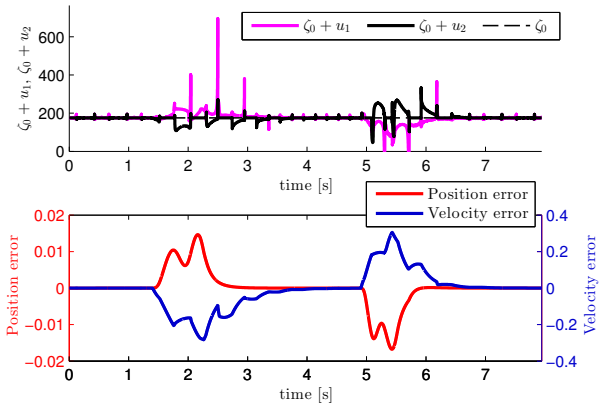

Fig. 8. Control input and error functions. The leg stiffness converges to a constant value after rejection of the transition disturbances. Note that during single-support, the stiffness of the swing leg is always equal to ζ_0, as $\tilde{u}_2 \equiv 0$ in that case (Eq. (17)–(18)).

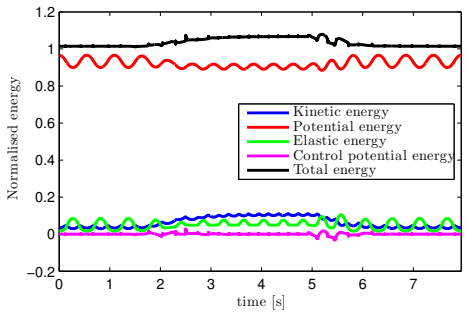

Fig. 9. Energy balance. The total energy increases on transition to the second gait, mostly reflected in kinetic energy resulting from the increased forward velocity.

generated by simplified Variable Stiffness Actuator (VSA) models (Sec. V-A). The foot contact points are denoted c_l, c_r, similar to the S-SLIP model. The ground contact forces are modeled using the Hunt-Crossley contact model. The robot is constrained to the sagittal plane using constraint forces.

A. *Variable Stiffness Actuator (VSA)*

Variable Stiffness Actuators (VSAs) belong to a class of actuators which are able to change their apparent output stiffness K independently of their output equilibrium position by proper control of their internal degrees of freedom $\mathbf{z}$ (Fig. 12).

The used design is based on the principle of a lever arm with length d, with a movable pivot of which the position is given by $z_1 \in [0, d]$ (Fig. 13), which changes the transformation ratio between change in output position and change in spring state. For the analysis we use the port-Hamiltonian method, using a Dirac structure. For more details, see [12]. For Fig. 13, the spring state $s(\mathbf{z})$ with $\mathbf{z} = [z_1, z_2]$ is given as

$$s = \frac{d}{q_1}(d - z_1)\sin(r - z_2) \tag{24}$$

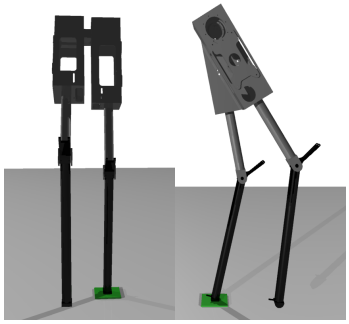

Fig. 10. The bipedal robot model is based on the mechanical design of a bipedal walker in our lab, with realistic body dynamics, friction and ground contact forces.

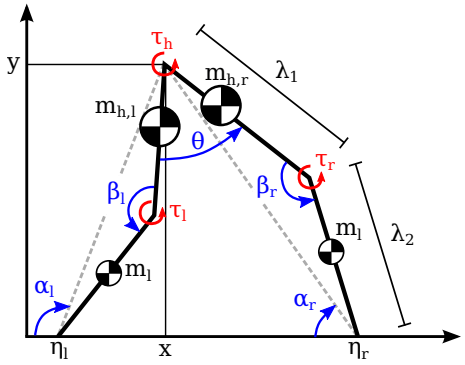

Fig. 11. Bipedal robot model. The model is similar to the S-SLIP model, with the hip mass replaced by two upper-leg masses and the addition of two lower-leg masses.

in which small deflections are considered, i.e. $r - q_2 \approx 0$:

$$s \approx \frac{d}{z_1}(d - z_1)(r - z_2) \tag{25}$$

The apparent output stiffness K of the actuator is then given by

$$K = k\frac{d}{z_1}(d - z_1) \tag{26}$$

where k is the stiffness of the internal spring. It is clear that for $z_1 = d, K \equiv 0$ and for $z_1 = 0, K \equiv \infty$. Eq. (26) is not a function of z_2, such that the equilibrium position

Fig. 12. Variable stiffness actuator with internal degrees of freedom $\mathbf{z} = [z_1, z_2]$. The stiffness K at the output link r is controlled independently of the equilibrium position z_2 by the stiffness controlling variable z_1.

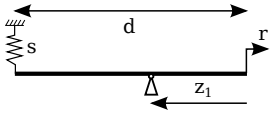

Fig. 13. Output stiffness changing mechanism based on the principle of changing the transformation ratio between an internal spring and the output link. A lever with length d with movable pivot z_1 connects the output r with an internal spring with stiffness k and state s.

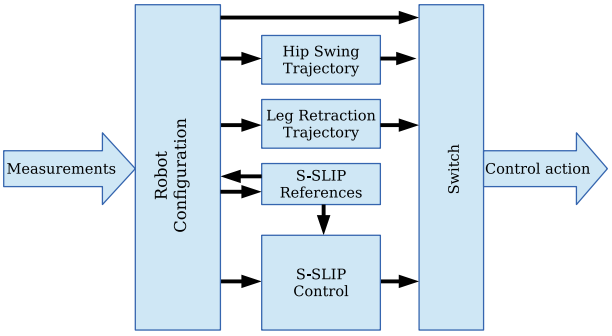

Fig. 14. Proposed controller structure. Joint angles and foot contact measurements are used to obtain the robot configuration and phase. The controller switches between constant-stiffness trajectory control or stiffness control of each of the knees depending on the phase. During leg swing, the hip and leg retraction trajectories are generated using minimum-jerk trajectories.

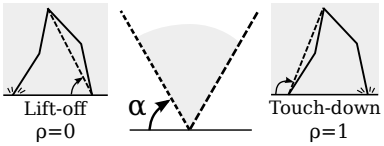

Fig. 15. During single-support phase the hip swing and leg retraction are parametrised using the variable ρ such that $\rho = 0$ at lift-off and $\rho = 1$ at the expected moment of touch-down.

and output stiffness can be easily be varied independently. For simplification and analysis of VSA requirements, we consider the control of z_1, z_2 such that they have asymptotic convergence to their desired set points.

VI. BIPEDAL ROBOT CONTROL DESIGN

A. Controller Structure

The proposed controller structure of the bipedal robot is shown in Fig. 14. The controller determines the robot configuration and phase from angle measurements and foot contact sensors. For the SS stance leg and DS, the controller uses stiffness control from the S-SLIP model. During stiffness control the equilibrium position of both knees is set to β_0, i.e. the knee rest angle, to obtain the desired S-SLIP variable spring behaviour. The swing leg is controlled using constant-stiffness trajectory control of the knee for leg retraction. The hip swing and leg retraction trajectories are generated using minimum-jerk trajectories, parametrised by a variable ρ (Sec. VI-B).

B. Step Parametrisation

For control of the hip swing and leg retraction, each step is parametrised from lift-off to subsequent touch-down using the variable ρ (Fig. 15). We define $\rho \equiv 0$ at lift-off, and $\rho \equiv 1$ at the expected moment of touch-down. We define ρ as a function of the angle-of-attack of the current stance leg α, set to either $\alpha = \alpha_l$ (left stance) or $\alpha = \alpha_r$ (right stance):

$$\rho = \begin{cases} 0 & \alpha \leq \alpha_{lo} \\ (\alpha - \alpha_{lo})/(\alpha_{td} - \alpha_{lo}) & \text{otherwise} \\ 1 & \alpha \geq \alpha_{td} \end{cases} \quad (27)$$

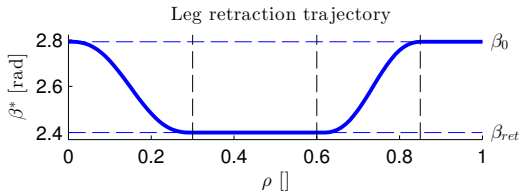

Fig. 16. Leg retraction trajectory for a rest knee angle of $\beta_0 = 160^o$. In our experiments, the retracted knee angle $\beta_{ret} = 2.4$ rad ≈ 137.5 deg.

such that given $\alpha_{td} > \alpha_{lo}$, $\rho \in [0, 1]$. We calculate $\alpha_{lo} = \alpha$ at the moment of lift-off to ensure continuous behaviour. The value of α at the expected moment of touch-down is obtained from the reference S-SLIP model as α_{td}. To ensure continuous behaviour, the value of ρ is also calculated during flight phase using the last stance leg.

C. Hip Swing

The desired hip trajectory $\theta^*(\rho)$ is generated using a minimum-jerk trajectory, with boundary conditions:

$$\begin{pmatrix} \theta^*(0) \\ \theta^*(1) \end{pmatrix} = \begin{pmatrix} \theta_{lo} \\ \theta_{td} \end{pmatrix} \quad (28)$$

Where θ_{lo} is the hip angle calculated at the moment of swing leg lift-off and θ_{td} is the hip angle expected to result in the desired angle-of-attack of the swing leg, calculated as $\theta_{td} = \alpha_0 - \alpha_{td}$.

D. Leg Retraction

The leg retraction trajectory is generated similarly to the hip swing. However, the leg is kept retracted for a period during the swing to avoid foot scuffing.[1] The desired knee angle β of the swing leg is given as

$$\beta^*(\rho) = \begin{cases} r_1(\rho) & 0 < \rho < 0.3 \\ \beta_{ret} & 0.3 \leq \rho \leq 0.6 \\ r_2(\rho) & 0.6 < \rho \leq 0.85 \\ \beta_0 & 0.85 < \rho < 1 \end{cases} \quad (29)$$

where β_{ret} is the retracted knee angle and $r_1(\rho), r_2(\rho)$ are minimum-jerk trajectories which control β^* from β_0 to β_{ret} and from β_{ret} to β_0 respectively (Fig. 16). In our experiments, $\beta_{ret} = 2.4$ rad ≈ 137.5 deg.

VII. BIPEDAL ROBOT MODEL RESULTS

The bipedal robot was modeled in the Controllab 20-sim software package using the Vode Adams integrator with absolute and relative tolerances of 1e-8. The system parameters are as in Table I.

A. Gait Reference

To obtain the gait reference for the bipedal robot model, the system was given a constant leg stiffness ζ_0 (i.e. stiffness control turned off) and a small push forward to start walking. This way the system only controls the required leg swing and leg retraction based on the value of ρ (Sec. VI-B), i.e. there

[1]Note that the moments of retraction and extension are tunable parameters which may affect the system performance depending on lower leg mass.

$m_{h,l}$	7.511	[kg]	m_l	0.779	[kg]
m_{h_r}	6.848	[kg]	ζ_0	196.6	[N m rad^{-1}]
λ_1	0.515	[m]	λ_2	0.495	[m]
β_0	160	[deg]	α_0	70	[deg]
β_{ret}	2.4	[rad]	α_{td}	98.3	[deg]

TABLE I

BIPEDAL ROBOT MODEL PARAMETERS

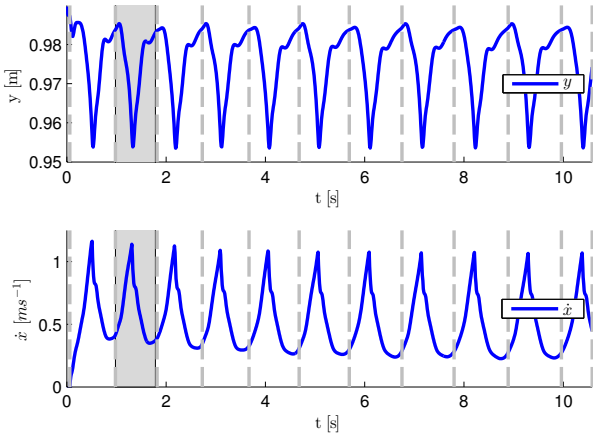

Fig. 17. Walking behaviour with constant leg stiffness. Vertical dashed lines indicate VLO. The shaded area indicates the step that was used for reference gait approximation. As there is no dependency on a reference the behaviour is mainly determined by leg swing dynamics. The average gait velocity is decreasing as time progresses, and, eventually, the system will come to a standstill.

is no dependency on some parametrised reference and the behaviour is mainly determined by leg swing dynamics. The resulting walking behaviour is shown in Fig. 17. Vertical dashed lines indicate VLO. The system starts in left stance, and there is a small difference between left and right stance due to the slightly different masses (Sec. V). It was found that walking gait is obtained for a range of leg swing angles in this way. It is observed that the additional dynamics of this system compared to the S-SLIP model results in a different velocity profile. As the swing leg slows down at the end of every swing, it pulls the hip forward which allows the forward velocity to increase quickly before touch-down. Compared to the S-SLIP model there is more variation of forward velocity during a single step.

Walking starts with an average forward velocity of ≈ 0.7 m s^{-1}, however the average gait velocity is decreasing as time progresses, and, eventually, the system comes to a standstill. Thus, only the hip swing is not injecting sufficient energy that is lost on impact and due to friction. We approximate the gait reference by the hip trajectory of the second step by Fourier series (shaded area in Fig. 17).

B. Walking Results

We now enable the S-SLIP knee stiffness controller. In (17)–(19) we set $\{\epsilon, \kappa_p, \kappa_d, \kappa_v\} = \{0.1, 50, 25, 50\}$. Fig. 18 shows the walking behaviour of the system after walking for some time. The system has converged to a stable walking gait with constant average gait velocity. The stiffness control

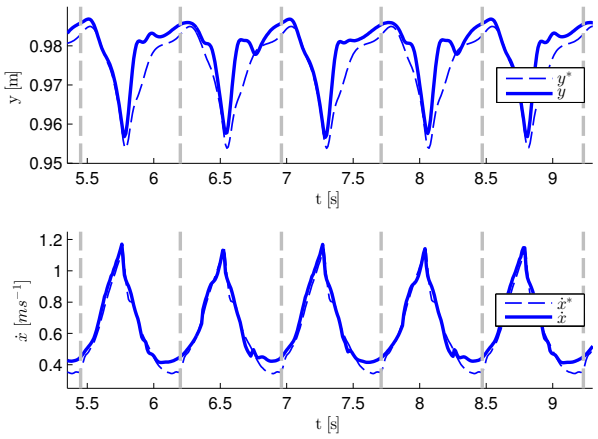

Fig. 18. Stable walking gait with controlled leg stiffness. The stiffness control successfully injects the lost energy every step such that the average gait velocity remains constant. Some asymmetry remains between left and right stance due to the mass difference.

successfully injects the lost energy every step such that the average gait velocity remains constant. Some asymmetry remains between left and right stance, due to the mass asymmetry (Sec. V). This is reflected in the inputs and errors (Fig. 19); as the reference was created out of a step during right stance there is a larger error and control inputs during left stance. The hip height error is below 1.5 cm and the velocity error is below 0.1 m s^{-1}. The control inputs are limited to $u_l, u_r \in [-\zeta_0, 1000]$ N m rad^{-1}.

The average forward velocity during the shown interval is 0.65 m s^{-1}, corresponding to a Froude number *Fr* of ≈ 0.21. In comparison, "Meta" [10] achieves speeds ranging from an *Fr* of 0.1 to 0.28, and "Veronica" [9] achieves an *Fr* of 0.07 to 0.16.

The SS velocity control law (18) generates high control inputs, especially during touch-down and left-foot push-off. This results from the orientation of the leg in these cases and low compression of the leg. It is likely these inputs could be smaller, as they do not influence forward velocity very much and significantly disturb hip height. During SS position control (Eq. (17)), close to VLO, the control inputs are generally small, as the reference was created out of the natural dynamics of the system and the hip height disturbance arising from foot push-off during velocity control is quickly rejected. The actuator power corresponding to the control inputs are shown in Fig. 20. Hip actuator power is below 60 W. VSA z_1 power is generally below 20 W. z_2 power has peaks up to 150 W due to the short leg retraction and extension time and low retraction angle (Fig. 16). These values are within the limits of the motors of the physical robot, although we did not account for efficiency overhead of the mechanical implementation of the VSAs [12].

Important to the performance of the system is the moment of touch-down. Due to the explicit dependency on a gait reference parametrised in x, disturbances to the system can result in the system running out of phase with the reference due to different moments of touch-down.

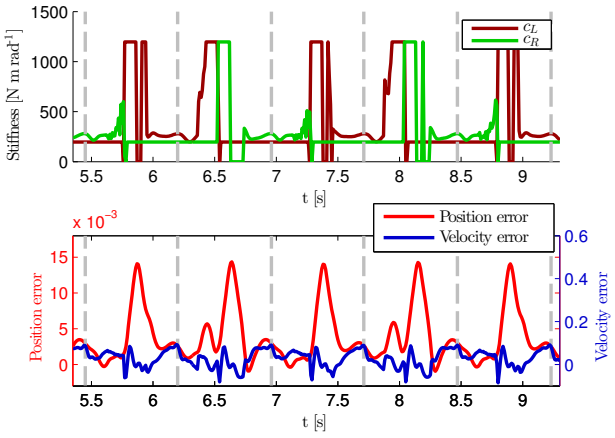

Fig. 19. Control inputs and errors. As the reference was created out of a step during right stance, there is a larger error and control inputs during left stance. The SS velocity control law (18) generates high control inputs, especially during touch-down and left-foot push-off. During SS position control (Eq. (17)) the control inputs are generally small, as the reference was created out of the natural dynamics of the system and the hip height disturbance arising from foot push-off during velocity control is quickly rejected.

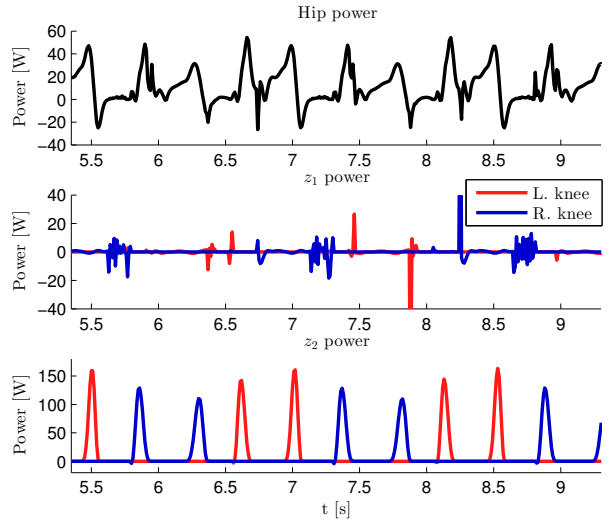

Fig. 20. Hip and VSA power. Hip power is below 60 W. VSA z_1 power is generally below 20 W. z_2 power has peaks up to 150 W due to the short leg retraction and extension time and low retraction angle (Fig. 16).

VIII. CONCLUSIONS & FUTURE WORK

We have analysed the dynamics of the S-SLIP system and developed a control strategy based on variable knee stiffness that is able to reject external disturbances to the system and can control the system from one limit cycle walking gait to another. It was shown that the controller can switch gait by injecting or removing energy from the system appropriately, after which control inputs converge to zero.

Based on this, a control strategy was developed that is able to stabilise a bipedal robot model with realistic dynamics into a stable walking gait. To obtain the desired S-SLIP variable stiffness behaviour together with adjustable knee equilibrium position for leg retraction, we use a variable stiffness actuator. The controller successfully injects energy losses generated by friction and foot impacts. At the moment just after touch-down and just after push-off, the chosen strategy does result in high control inputs. This is due to the current leg orientation and low compression of the leg. We suspect these inputs could be smaller, as it does not influence forward velocity very much and significantly disturbs hip height.

The controller takes into account the additional dynamics of the bipedal robot model such as hip swing and leg retraction. The gait reference was obtained from the constant-stiffness walking behaviour of the system. Our results showed that the moment of touch-down is important, mainly due to the explicit dependency on a gait reference parametrised in forward position. In the case of disturbances or inappropriate leg swing this may lead to the system running out of phase with the reference. A future control strategy should therefore be based on the current state of the system as much as possible, perhaps by parametrisation of the reference w.r.t. measured touch-down events. Additionally, an active hip swing set point generation strategy, perhaps inspired by [8], should be considered that adjusts the angle-of-attack of the swing leg on-line.

Furthermore, more limit cycle gaits on the bipedal robot model should be explored. In the current results high knee stiffness was used to obtain a reference gait, however gaits with lower leg stiffness could make better use of the compliant leg behaviour. Additionally, the leg swing behaviour could be varied further.

REFERENCES

[1] T. McGeer, "Passive dynamic walking," *The International Journal of Robotics Research*, vol. 9, no. 2, pp. 62–82, 1990.

[2] S. Collins and A. Ruina, "A bipedal walking robot with efficient and human-like gait," *Robotics and Automation (ICRA), 2005 IEEE International Conference on*, 2005.

[3] H. Geyer, A. Seyfarth, and R. Blickhan, "Compliant leg behaviour explains basic dynamics of walking and running," in *Proceedings. Biological sciences / The Royal Society*, vol. 273, no. 1603, pp. 2861–7, 2006.

[4] J. Rummel, Y. Blum, and A. Seyfarth, "Robust and efficient walking with spring-like legs," *Bioinspiration & Biomimetics*, vol. 5, no. 4, p. 16, 2010.

[5] J. Rummel and A. Seyfarth, "Stable Running with Segmented Legs," *The International Journal of Robotics Research*, vol. 27, no. 8, pp. 919–934, 2008.

[6] L. C. Visser, S. Stramigioli, and R. Carloni, "Robust Bipedal Walking with Variable Leg Stiffness," in *Proceedings of the 2012 4th IEEE RAS & EMBS International Conference on Biomedical Robotics and Biomechatronics (BioRob)*, pp. 1626–1631, 2012.

[7] J. G. Ketelaar, L. C. Visser, S. Stramigioli, and R. Carloni, "Controller design for a bipedal walking robot using variable stiffness actuators," Robot. Autom. (ICRA), 2013 IEEE International Conference on, pp. 5650–5655, 2013.

[8] H. R. Martinez Salazar and J. P. Carbajal, "Exploiting the passive dynamics of a compliant leg to develop gait transitions," *Physical Review E*, vol. 83, no. 6, p. 066707, 2011.

[9] Y. Huang, B. Vanderborght, R. Van Ham, Q. Wang, M. Van Damme, G. Xie, and D. Lefeber, "Step Length and Velocity Control of a Dynamic Bipedal Walking Robot With Adaptable Compliant Joints," *IEEE/ASME Transactions on Mechatronics*, vol. 18, no. 2, pp. 598–611, 2013.

[10] D. G. E. Hobbelen and M. Wisse, "Controlling the Walking Speed in Limit Cycle Walking," *The International Journal of Robotics Research*, vol. 27, no. 9, pp. 989–1005, 2008.

[11] S. V. Kuznetsov, "The motion of the elastic pendulum," *Regular and Chaotic Dynamics*, vol. 4, no. 3, pp. 3–12, 1999.

[12] S. S. Groothuis, G. Rusticelli, A. Zucchelli, S. Stramigioli, and R. Carloni, "The vsaUT-II: a Novel Rotational Variable Stiffness Actuator," *2012 IEEE Int. Conf. Robot. Autom.*, pp. 3355–3360, 2012.

4 Conclusions

The efforts that led to this master thesis have been the investigation of the control of bipedal walking robots based on the principle of passive dynamic walking. The goal has been to use variable leg stiffness to obtain variable walking gait, while combining two goals that have thus far been hard to realise simultaneously in walking systems – robustness and energy-efficiency.

Two conceptual models have been analysed – the Spring-Loaded Inverted Pendulum (SLIP) and Segmented Spring-Loaded Inverted Pendulum (S-SLIP) models – that are some of the simplest models that exhibit walking gait using compliant elements. Much of the initial work focused on exploring the parameter space of the SLIP model, specifically, the achievable velocity ranges given different combinations of system parameters. It was found that for many desired velocities a range of gaits exists that can achieve the desired velocity. Normalised descriptions of these *natural gaits* – limit cycle walking gaits – were developed for both the SLIP and S-SLIP model, which allows for comparison of gaits across systems with different parameters.

Control strategies were developed for the systems that were able to stabilise their walking gaits, and control the systems from one limit cycle walking gait to another. Linear interpolation between two gait trajectories and their corresponding stiffness values and angles-of-attack during transition was shown to be a successful strategy to change between gaits which have different angles-of-attack. The results show that the concept of variable leg stiffness is not only suited to stabilising a walking model into its existing gait, but also to inject or remove energy from the system appropriately to switch between gaits, for example to change to a desired velocity.

Based on this work a bipedal robot model with realistic dynamics was developed that uses Variable Stiffness Actuators (VSAs) to control the knees and thus leg stiffness. The S-SLIP control strategy was used, extended with additional components to facilitate hip swing and leg retraction arising from the additional dynamics.

Initial attempts at controlling the bipedal robot model used a reference obtained from the S-SLIP model. However, the additional dynamics of the bipedal robot model required very high control gains and well-tuned leg swing angles to result in stable gait. The result was not robust and the large control inputs made the solution infeasible. It was therefore concluded that the dynamics of the S-SLIP model are not close enough to that of our bipedal robot model to enforce its behaviour as a reference. It was found that on the bipedal robot model there exist walking patterns when using constant leg stiffness (i.e. without using stiffness control). However, energy losses did not allow the system to converge to a limit cycle walking gait. The stiffness control strategy developed for the S-SLIP model was shown to be able to successfully inject the energy losses and stabilise the system into a limit cycle walking gait.

The goal of energy efficiency has not been thoroughly addressed in this work. The gait reference was constructed such to attempt to use the passive dynamics of the system as much as possible. However, while the power delivered by the hip and VSAs was generally low and within actuator constraints for the physical system, the control has not been optimised for energy efficiency. It is expected that by further development of the control architecture and appropriate references the energy efficiency of the system can be significantly improved.

5 Recommendations

- The gait switching strategy developed for the SLIP and S-SLIP models performs well, however robustness should be analysed further. For example, it appears there are limits to the maximally allowable difference in angle-of-attack between the two gaits. In this case, an intermediate gait could be used in the interpolation to further stabilise the system.

- Neither the SLIP system nor the S-SLIP system exhibits limit cycle walking gaits that are similar to the walking behaviour obtained from the bipedal robot model with constant knee stiffness. Enforcing their behaviour on the bipedal robot model therefore does not seem like a viable direction. A deeper exploration of the parameter space that leads to limit cycle walking gaits on the bipedal robot model is essential in order to reach the combined goal of robust, energy efficient walking. Specifically, gaits with lower nominal knee stiffness than were shown here may lead to better use of the internal energy storage and greater controllability of the system.

  Additionally, adding a feed-forward foot push-off term may lead to limit cycle walking gaits that are self-stable (i.e. the push-off injects the energy otherwise lost to friction and foot impacts) without using the S-SLIP based knee stiffness control. In this case adding the S-SLIP controller would improve robustness and allow control action to converge to zero, similar to the S-SLIP simulation results.

- The variable stiffness actuator design inspired by the vsaUT-II appears to be suitable for control of the bipedal robot. The power requirements are below the specifications of the physical system, although the model was linearised for small deflections around its equilibrium point and efficiency losses due to the specific mechanical implementation have not been taken into account. Before implementation on the real set-up a more detailed requirements study is necessary. From previous work it is known that there may be problems with the current VSAs to adjust the stiffness while the actuator is loaded. To negate this issue, an additional parallel spring could be added to the actuators that unloads the VSA lever structure and provides a minimum stiffness value.

- We attempt to obtain energy efficiency by using the passive dynamics of the system as much as possible. However, despite the use of VSAs, their control during stance was not optimised for energy efficiency. Instead, they are controlled as pure variable stiffness elements to obtain behaviour comparable to the S-SLIP model. However, by controlling both internal degrees of freedom appropriately, it is possible to adjust the output stiffness of a loaded VSA without changing the energy stored in the internal compliant element. Doing so may increase the energy efficiency of the bipedal robot control as a whole.

- The present control architecture of the bipedal robot model explicitly depends on a gait reference parametrised in the forward position of the robot. This results in a large dependency on the exact moment of touch-down, which leads to problems in the case of external disturbances to the system or inappropriate leg swing. Running out of phase with the reference eventually leads to loss of performance or falling of the robot. A gait reference could for example be parametrised w.r.t. the last double-support phase, the angle-of-attack of the current stance leg, or touch-down or lift-off events.

- In the current control architecture, the hip is always swung to the same angle before touch-down. An active hip swing set point generation strategy, that adjusts the angle-of-attack of the swing leg on-line on every step, may be beneficial in terms of gait stabilisation and switching of gaits, e.g. by putting the foot more forward to slow down.

A Appendix: 20-sim models

In this appendix we describe the 20-sim model structure.

A.1 Main model

Fig. 1 shows the top-level view of the model. The 3D mechanics model (*'clw'*) implements the walker 3D dynamics, and provides force/torque inputs and measurement outputs by which the rest of the model interacts with the mechanics. The 3D mechanics model is shown in Fig. 2. The constraint forces shown in Fig. 1 prevent the walker from moving out of the sagittal plane (which is aligned with the x-z plane) or rotate around the x- and z-axes, respectively.

Shown in the top-right are the initial push forces, which act in the first simulated second to initiate walking. The z-push was turned off in our experiments, and the x-push was 10 N for 0.5 s. Shown in the bottom-right are the ground reaction forces, which implement the Hunt-Crossley contact model and friction to prevent foot sliding.

Shown just left of the centre are the actuators, joint friction and end stops. The knee end stops were modeled as a spring-damper at knee angles of 1.0 rad (≈ 57 deg) and 2.9 rad (≈ 166 deg), respectively. The *'VSA_L'* and *'VSA_R'* blocks implement the Variable Stiffness Actuator (VSA) models, described in the next sections. The hip actuator is modeled as an electric motor with gearbox as in the physical system, with the *'Low_Level_IO'* block implementing the required conversion from desired hip torque to motor current. Shown left is the *'Controller'* submodel, detailed in the next section.

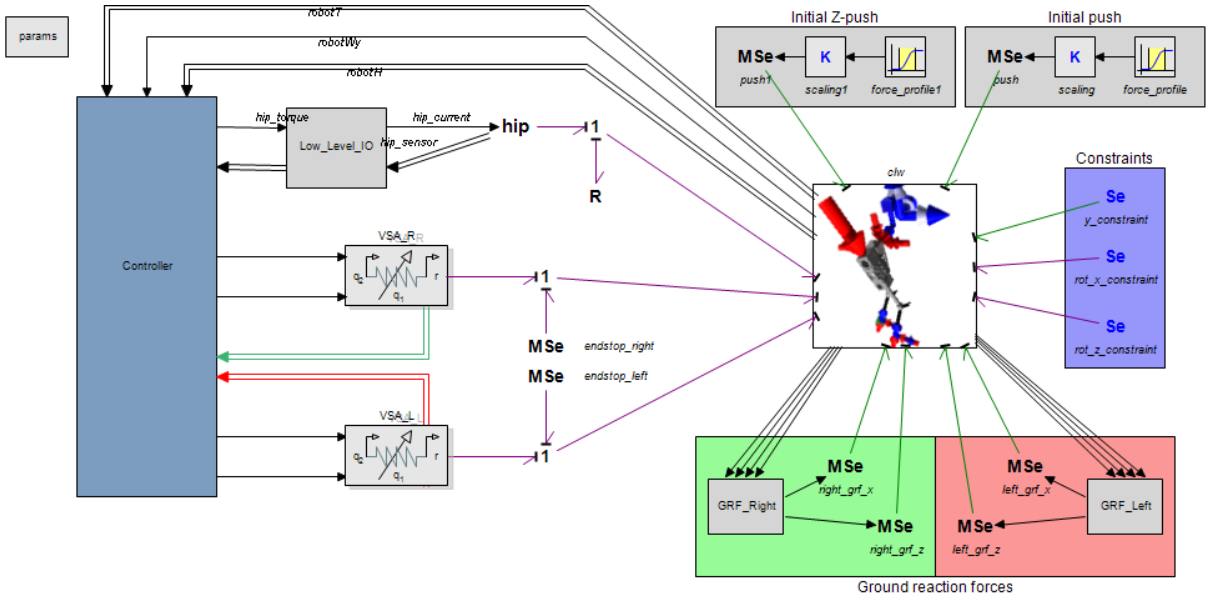

Figure 1: Top-level overview

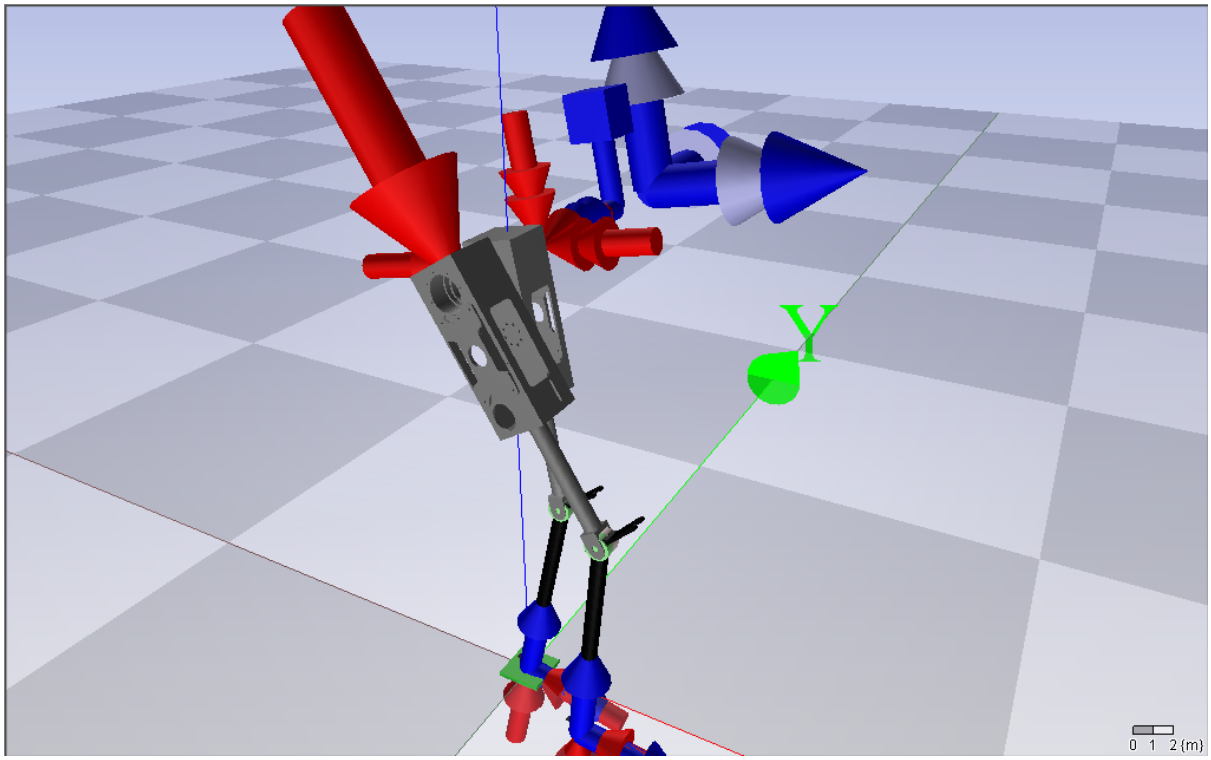

Figure 2: 3D mechanics model

A.2 Controller

The controller structure is shown in Fig. 3. The controller receives position, attitude and velocity measurements of the hip, as well as hip and knee measurements in the *'RobotConfiguration'* submodel. This submodel calculates the current robot state, the phase (single-support (SS) or double-support (DS) respectively) as well as ρ (see paper 2), foot contact positions, and angles-of-attack.

The *'S_SLIP_References'* submodel describes the gait reference for use by the S-SLIP controller, as well as provide values for the hip angle which is expected to lead to the desired angle-of-attack at touch-down. Using these values, the *'S_SLIP_Control'* block calculates the desired torsional knee stiffness for each of the legs during stance.

Additional components which facilitate hip swing and leg retraction are implemented in the *'hipControl'* and *'retractControl'* submodels. Using the phase and value of ρ, they generate the appropriate minimum-jerk trajectories. The *'Switch'* block switches between the S-SLIP knee stiffness control and trajectory following for each of the legs depending on the phase, and controls the hip swing during single-support phase. During S-SLIP knee stiffness control, the VSA equilibrium position is set to the rest angle of the knee to obtain the desired S-SLIP variable knee stiffness behaviour.

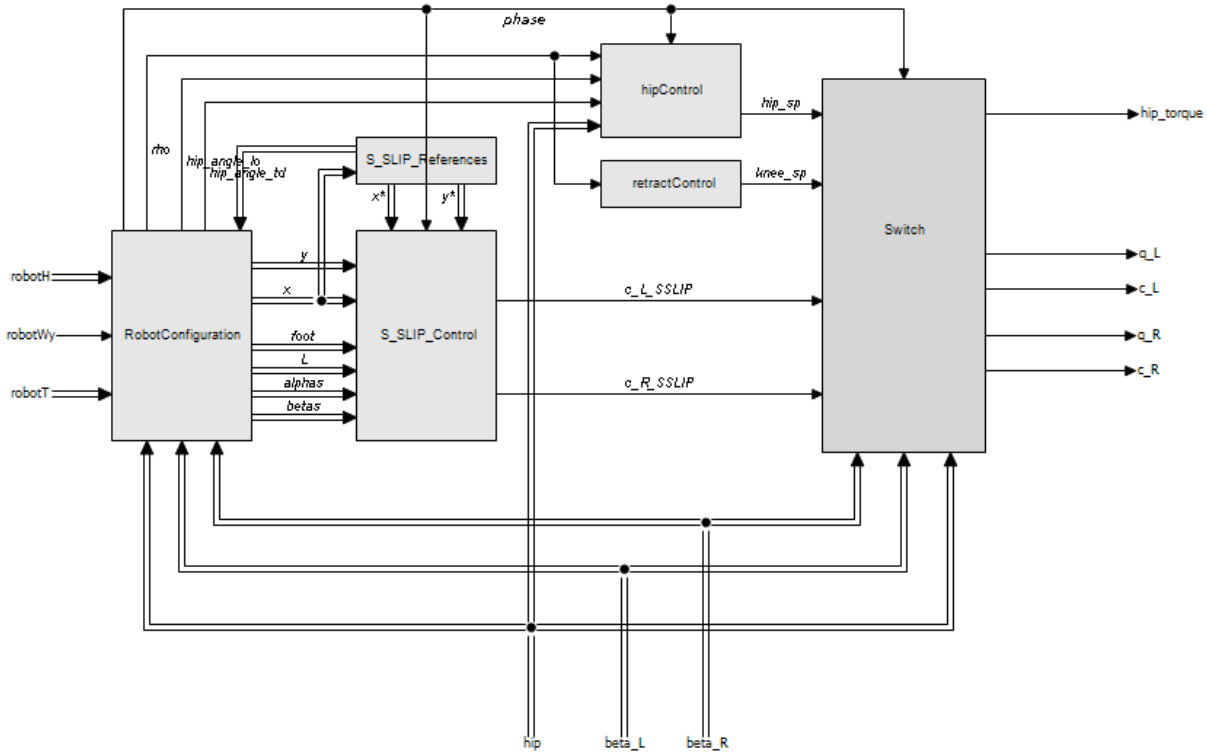

Figure 3: Controller structure

A.3 Variable Stiffness Actuator (VSA) model

The VSAs were implemented using the lever arm design of the vsaUT-II, which varies its stiffness based on the change of the transmission ratio between the output link and an internal compliant element. The model of the VSA used in our simulations is shown in Fig. 4. Note that the model is linearised for small deflections around its equilibrium position, and does not include efficiency losses due to the specific mechanical implementation. The desired value of the pivot point q_1 is calculated from the desired stiffness `k_star`, and is controlled to its desired setpoint exponentially using a flow source (which approximates an ideal servo motor) inside the *'q1_control'* submodel. The equilibrium position q_2 is controlled similarly with exponential convergence to its desired position. The *'init'* submodel initialises all initial positions and calculates the initial spring state from them (allowing the VSA to be loaded at $t = 0$).

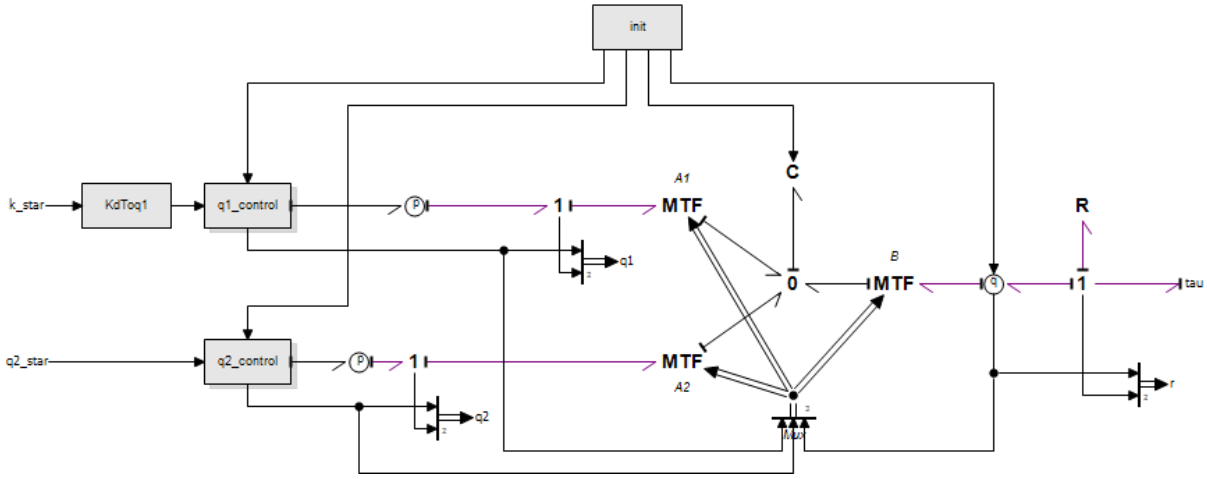

Figure 4: Variable Stiffness Actuator (VSA) model showing the Dirac structure.